이학박사 학위논문

알츠하이머 질환 모델에서 와베인의 Transcription factor EB의 활성화를 통한 신경세포 보호

Transcription factor EB activation and neuro-protection by ouabain in Alzheimer's disease models

울 산 대 학 교 대 학 원

의 학 과

송 하 림

Transcription factor EB activation and neuro-protection by ouabain in Alzheimer's disease models

Superviser : Kim Dong Hou

A Dissertation

Submitted to
the Graduate School of the University of Ulsan
In Partial Fulfillment of the Requirements
for the Degree of

Doctor of Philosophy in Science

by

Ha-Lim Song

Department of Medicine
Ulsan Korea

August 2019

Transcription factor EB activation and neuro-protection by ouabain in Alzheimer's disease models

This certifies that the dissertation

of Ha Lim Song is approved.

Committee Vice-chair Dr. Seung-Yong Yoon

Committee Member Dr. Dong-Hou Kim

Committee Member Dr. Yeon Jin Jang

Committee Member Dr. Han Seok Choe

Committee Member Dr. Kyung Hoon Hwang

Department of Medicine

August 2019

Abstract

The neurofibrillary tangles containing abnormal hyperphosphorylated tau protein correlates with the degree of dementia in Alzheimer's disease (AD). In addition, features of autophagosome accumulation and damage due to autophagy, a degradation process of toxic protein aggregation in the cytosol, are also found in AD brain. These features indicate that regulation of the autophagy-lysosome system could be a therapeutic strategy for AD. Activation of Transcription factor EB (TFEB), a master regulator of autophagy-lysosome system gene transcription, reduces the amount of tau in transgenic mice that overexpress amyloid precursor protein (APP mice). Here, to search for therapeutic compounds for AD, it conducted two kinds of screening to identify pharmacologically active compounds that increase 1) neuronal viability in okadaic acid-induced tau hyperphosphorylation-related neurodegeneration models and 2) the nuclear localization of TFEB in high-content screening. Ouabain, a cardiac glycoside, was discovered as a common-hit compound in both screenings. It also exhibited significant protective effects in tau transgenic fly and mouse models in vivo. Through inhibition of the mechanistic target of rapamycin (mTOR) pathway and activation of TFEB, ouabain enhances downstream autophagy–lysosomal gene expression and cellular restorative properties and reduces phosphorylated tau in vitro and in vivo. This study reports the effects of ouabain as a promising therapeutic to modulate autophagy through the activation of TFEB and reduce the accumulation of abnormal toxic tau.

Keyword**:** Alzheimer’s disease, Okadaic acid, Transcription factor EB, Tau, Ouabain, mTOR

Contents

List of Figures

Abbreviations

AD: Alzheimer's disease

NFTs: neurofibrillary tangles

Aβ: β-amyloid peptide

APP: amyloid precursor protein

TFEB: Transcription factor EB

OA: Okadaic acid

LOPAC^{1280}: the 1,280-compound Library of Pharmacologically Active Compounds

DMEM: Dulbecco's modified Eagle's medium

GFP: green fluorescent protein

PBS: phosphate-buffered saline

FITC: fluorescein isothiocyanate

LDH: lactate dehydrogenase

MTT: 3-(4,5-dimethylthiazol-2-yl)-2,5-diphenyltetrazolium bromide

p-tau: phosphorylated tau

mTORC1: mechanistic target of rapamycin complex 1

dMitf: microphthalmia-associated transcription factor

dMitfKD: knockdown of dMitf

WT: wild-type

1. Introduction

The alzheimer's disease (AD) is accompanied by atrophy phenomenon in brain, and eventually leads to death. The main pathologic elements of the disease are neurofibrillary tangles (NFTs) and senile plaques (1, 2). NFTs are formed by intra-neuronal accumulation of paired helical filaments composed of abnormally hyper-phosphorylated tau protein. Senile plaques contain β-amyloid peptide (Aβ), which arises through proteolytic processing of amyloid precursor protein (APP) by two site-specific proteases: β-secretase and γ-secretase.

The current medication helps to cover the symptoms rather than treating the underlying disorder or delaying the progression of AD. This is related to the failure of many studies and clinical trials targeting Aβ, one of the pathologic elements of AD. Recently, the other major pathogenic molecule, tau, focus as a therapeutic target for AD and other neurodegenerative diseases (3). In fact, the pathology of NFT containing abnormal hyper-phosphorylated tau is more consistent with the Braak stage, which plaque and tangle distribution at AD progression (1, 4, 5).

The physiological role of tau binds to microtubules and supports its function, during the tauopathy, proteases cleave both 3- and 4-repeat tau to produce neurotoxic fragments (6, 7). Proteolytic fragments of tau can have increased trend to be phosphorylated and aggregate into neurofibrillary tangles. Fragments of tau can cause its separation from the microtubules, which potentially lead to microtubule collapse (8). These phenomena lead to the synaptic and neuronal loss to support tauopathy-associated neurodegeneration. Tau-directed therapeutics included the following methods for relieving the neurotoxic gain of tau function or the loss of tau function (9). These methods contain tau reduction (10, 11), inhibition of tau phosphorylated and aggregation (12, 13), microtubule stabilizers (14, 15), and immunotherapy using tau-specific antibodies (16, 17). In addition, there is protein quality control that is induced through proteasome or autophagy as a major role to prevent tau

aggregation and reduce toxic tau, which can promote refolding or degradation of misfolded tau (18-20).

The disturbance of autophagy is believed to play an important role in AD pathophysiology, and autophagy has gained interest as a therapeutic target (21). Autophagy regulates cellular homeostasis by degrading toxic protein aggregates in the cytosol through fusion with lysosomes (22). Many features related to autophagy disturbance, such as autophagosome accumulation and lysosomal dysfunction, were reported in AD models (23). This means lysosome fusion and degradation in the late stage of autophagy are important for substrate clearance (24) and suggests that strengthening the autophagy-lysosome system may be considered as a treatment strategy for AD (25-27).

Transcription factor EB (TFEB) is the master regulator of the autophagy-lysosome system (28). TFEB is present in its phosphorylated form in cytosol, but under special condition environment, such as starvation, it is dephosphorylated and translocated to the nucleus, where it initiates transcription of genes involved in autophagy and lysosome machineries (29). The autophagy-lysosome system induces degradation of abnormal proteins not only by autophagy but also lysosomes (30). In APP/PS1 mice of AD amyloidosis, the enhancement of TFEB increases the level of autophagy-lysosome related proteins and decreases phosphorylated tau (31).

Okadaic acid (OA), a protein phosphatase 2A inhibitor, induces hyper-phosphorylated tau and cell death in neurons (32, 33). OA leads to pathological progression *in vivo* similar to AD and subsequent neuronal degeneration, synaptic loss, and memory loss (34, 35). Thus, the OA-induced neurodegeneration model is useful for studies involving tau phosphorylation in the neuronal degeneration process.

In this study, the 1,280-compound Library of Pharmacologically Active Compounds

(LOPAC^{1280}) were screened and identified that ouabain, a cardioactive glycoside composed of rhamnose and ouabagenin (36), protected against cell damage induced by OA in neurons and induced autophagy pathway via TFEB activation. Ouabain also resulted in the reduction of phosphorylated tau, improving a rough-eye phenotype of a *Drosophila melanogaster* tau model as well as memory performance in Tau-P301L mice.

2. Materials and Methods

2. 1. Reagents

Approximately 1,280 compounds are listed in the LOPAC® (Sigma–Aldrich, St Louis, MO, USA), spanning a broad range of cell signaling and neuroscience areas of activity. Okadaic acid, ouabain, MG132, and bafilomycin A1 were purchased from Sigma-Aldrich. Hoechst 33342, LysoTracker Red DND-99, and phalloidin were obtained from Invitrogen (CA, USA).

2. 2. Antibodies

The following antibodies and reagents were used. TFEB for human (cat. 4240, 1:1000), histone H3 (D1H2) (cat. 4499, 1:2000), p-mTOR(S2448) (cat. 2971, 1:1000), mTOR (cat. 2983, 1:1000), p-P70S6K Thr389 (cat. 9234, 1:1000), P70S6K (cat. 2708, 1:1000), p4EBP1-Thr37/46 (cat. 2855, 1:1000) and 4EBP1 (cat. 9644, 1:1000) were from Cell Signaling Technology. LC3B (L7543, 1:1000) and beta-actin (A5441, 1:3000) were from Sigma. MAP2 (AB5622, 1:100) was from Chemicon. TFEB for human and mouse (A303-673A, 1:1000) was from Bethyl Laboratories. GAPDH (MAB374, 1:2000) was from Millipore. LAMP1 (ab13523, 1:1000) was from Abcam. p-Tau199/202 (44-798G, 1:1000) and p-TauThr231(AT180, MN1040, 1:1000) were from Invitrogen. p-TauSer396(44-736, 1:1000) was from Biosource. Tau5 (MAB3420, 1:2000) was from Calbiochem.

2. 3. Cell culture and transfection

Primary cortical neuron culture was performed as described before (37). HeLa and SH-SY5Y cells were cultured in Dulbecco's modified Eagle's medium (DMEM, Hyclone) with 10% fetal bovine serum. All cells were cultured in a 5% CO_2 atmosphere at 37°C. Cells were transiently transfected with DNA plasmids: Human full-length TFEB-NT-GFP (pcDNA5 vector) from ADDGENE, and GFP-TauP301S using Lipofectamine-2000 from Invitrogen, according to the protocol from the manufacturers.

2. 4. High-throughput ATP assay screening

Primary cortical neurons were seeded in 96-well plates (655098, Greiner Bio-One). Compounds (2 μM) were added to neurons (DIV10), and after 30 min, OA (10 nM) was added, followed by incubation for 24 h. Cells were then washed with phosphate-buffered saline (PBS), and ATP activity was determined immediately using CellTiter-Glo® Luminescent Cell Viability Assay (Promega), according to the manufacturer's guidelines on a Perkin Elmer plate reader. The approximately 15,000 cells were analyzed for each experimental condition and the raw luminescence values were normalized using negative (DMSO treated) and positive (OA treated) controls in the each plate. The converted data was then normalized using Equation 1. Normalized well values were then corrected for position artifact based on proprietary pattern detection algorithms. Finally, robust Z-scores were calculated using Equation 2.

Equation 1.

$$\text{Normalized data} = \frac{\text{Converted data}_{\text{sample}} - \text{Median of converted data}_{\text{DMSO}}}{|\text{Median of converted data}_{\text{OA}} - \text{Median of converted data}_{\text{DMSO}}| \times 100}$$

Equation 2.

$$\text{Robust Z score} = \frac{\text{Converted data}_{\text{sample}} - \text{Median of converted data}_{\text{all sample}}}{\text{Converted robust standard deviation}_{\text{all sample}}}$$

For the primary screen, each compound was tested as N=1, and primary hits were selected with robust Z-scores less than 4. For the validation screen, the primary hits were assayed in triplicated. For each compound, the normalized activity values were condensed to a single value (condensed activity score) using the "Robust Condensing" method (38). The condensed activity is the most representative single value of the triplicates. Six compounds

with highest condensed activity values and robust Z-score values were selected as the hits.

2. 5. High-content GFP-TFEB chemical screening

HeLa cells-transfected with TFEB-GFP were incubated in 384-well black plates (Greiner Bio-One) for 12 h, and treated using each compound for 8 h in 5% CO_2 at 37°C. Cells were fixed with 4% formaldehyde and stained with Hoechst 33324. For the acquisition of images, at least 9 fields were prepared per well in the 384-well plate by using confocal automated microscopy (Opera high-content system; Perkin-Elmer, 20× objective). The analysis of TFEB localization was performed on different images (Harmony and Acapella software; Perkin-Elmer) using 405 and 488 nm laser lines with DAPI (4', 6-diamidino-2-phenylindole) and FITC (fluorescein isothiocyanate) emission filters. Briefly, nuclei were segmented using the Hoechst channel and the cytosol was segmented using the FITC channel. These calculate the ratio of the average numbers of cells with nuclear TFEB-GFP fluorescence divided by the average numbers of total cells with TFEB-GFP fluorescence. On average, approximately 8,000 HeLa cells were analyzed in this screening and the results were normalized using negative (DMSO treated) and positive (starvation) controls in the same plate. The same method as mentioned above was used to generate the seven compounds with highest condensed activity values and robust Z-score values as the hits.

2. 6. Lactate dehydrogenase (LDH) assay

Primary cortical neurons were plated in a 96-well plate with a white wall and a clear bottom. After 24 h of OA (10 nM) treatment, cell injury in DIV10 neurons was quantitatively assessed by measuring the LDH activity released into the bathing medium from damaged cells, using a CytoTox 96® NonRadioactive Cytotoxicity assay kit (G1780, Promega), according to the manufacturer' guidelines. Absorbance was measured spectrophotometrically at 490 nm in Tecan Infinite® 200 PRO.

2. 7. 3-(4,5-dimethylthiazol-2-yl)-2,5-diphenyltetrazolium bromide (MTT) assay

After 24 h of OA (10 nM) treatment, cell viability in DIV10 neurons was assessed using the MTT (Thiazolyl Blue Tetrazolium Bromide, Sigma Aldrich) reduction assay, using the manufacturer's guidelines. Absorbance was measured spectrophotometrically at 540 nm in Tecan Infinite® 200 PRO.

2. 8. Immunocytochemistry

Immunocytochemistry was performed according to protocol previously (37). After fixation, cell membranes were permeabilized by incubation with blocking buffer (1% Triton x-100, 5% goat-serum, 1% bovine serum albumin in PBS). Cells were incubated with primary antibodies at 4°C and followed by secondary antibodies for 1 h at room temperature. Cells were then treated with Hoechst stained and mounted on glass slides with mounting medium (Daco). All digital images were made using a 40X objective on a Nikon microscope and were further processed using NIS-Elements (Nikon Instruments Inc.). Ten images were evaluated for each sample, and three independent experiments were performed to generate the graphed values. F-actin was visualized with Rhodamine phalloidin (R415, Invitrogen) according to the manufacturer's guidelines.

2. 9. Neurite length

Cultured primary cortical neuron cells were treated with OA for 24 h or ouabain for 8 h, or were untreated. Cells were then fixed with 4% formaldehyde and stained with Hoechst 33342 and MAP2 antibodies according to the immunocytochemistry protocol. All images were made using a 20X objective on a Nikon microscope and were further processed and measured the neurites length on the NIS software. The analysis of neurite length was performed from MAP2-stained images for a total of 40 images (number of cells >200).

2. 10. Nuclear/cytosolic fraction

Cells transfected with TFEB-GFP were cultured in 6-well plates and treated with ouabain or remained untreated. Subcellular fractionation was carried out as follows: cells were lysed in Triton x-100 lysis buffer (50 mM Tris-HCl, 0.5% Triton x-100 supplemented with protease and phosphatase inhibitors in PBS). After 10 min, the lysate was centrifuged at 4°C. The supernatant consisting of the cytosolic fraction and pellet (nuclear fraction) was washed twice, lysed in buffer, and sonicated.

2. 11. Western blot

Western blots were performed according to standard methods under denaturing and reducing conditions. Briefly, samples were homogenized in lysis buffer containing phosphatase inhibitor cocktail (#P2850, Sigma-Aldrich, St. Louis, MO, USA) and protease inhibitors (#P8340; Sigma-Aldrich). Protein samples were separated on SDS-PAGE. Blots were incubated overnight at 4°C with the primary antibodies. Band analysis was performed using ImageJ software (National Institutes of Health, Bethesda, MD, USA).

2. 12. Staining for lysosome

The cells were stained with 500-nM LysoTracker^{TM} Red DND-99 (L7528, Invitrogen) according to the material's guideline. After staining, cells were washed 3 times with PBS and fixed in 4% paraformaldehyde.

2. 13. Experiments on using drosophila

2. 13. 1. Transgenic fly stocks and maintenance

The transgenic flies were regularly grown and maintained at 25°C and 60% humidity on a 12-h light-dark cycle and a standard cornmeal medium (recipe by Bloomington Drosophila Stock Centre, [BDSC], Bloomington, Indiana, USA). It obtained D. melanogaster elavc155-

GAL4 (#25750) and GMR-Gal4 (#1104) lines from BDSC. In this research work BestGene Inc. (MA, USA) generated Tau-transgenic flies (UAS-htau2N4RP301L) and dMitf-knockdown (UAS-MitfKD), by insertion at the attP site in the VIE260B genetic background, a fly line used to generate the VDRC-KK collection 23. The flies were backcrossed all lines for at least five generations to a w1118 line (#60000, VRDC), a well-known fly control line with normal circadian rhythm, learning, and memory.

2. 13. 2. *D. melanogaster* rough-eye phenotype

Up to 100 GMR-Gal4 transgenic virgins were crossed to UAS-Tau^{WT}, UAS-Mitf^{KD} male flies. Five days post egg-laying, it was collected up to 50 age-matched larvae from each genotype and incubated them at 27°C in standard fly food containing ouabain or solvent (Oua 2 μM and Oua 20 μM or 0.05% DMSO). It was collected male and female progeny 5–10 d PE and assessed light stereomicroscope images of their eyes for the presence of the rough-eye phenotype, using the 5 MP color digital camera. The fly-eye images were analyzed in ImageJ software (NIH) and calculated the eye size.

2. 13. 3. D. *melanogaster* survival assay

elavc155-Gal4 virgins were collected, sorted into batches of 50–100 flies, and crossed with age-matched males (wild w1118 and UAS-dMitfKD transgenic lines as well as UAS-tau and UAS-tau, UAS-dMitfKD), to produce the desired genotypes. At least 120 male flies per genotype (expressing one copy of tau transgene) were collected at d 0–1 PE and aged on standard cornmeal food (Bloomington recipe) complemented with 1.0 % agar. Each vial (9.5 × 2.4 cm) was kept on its side at 25°C and 60% humidity under a 12-h light-dark cycle. The number of flies per vial was optimized to 25, to avoid any mortality unrelated to phenotype. The fly food was exchanged every 2-3 days and the dead flies were collected and counted. The differences in survival were analyzed by the Kaplan-Meier equation in GraphPad Prism

5 (GraphPad Software, Inc., La Jolla, CA).

2. 14. Experiments on using Mouse

2. 14. 1. Mouse maintenance

The transgenic mouse was used TauP301L mouse, a well-characterized model of tauopathy (39-41). TauP301L mice originated from Taconic Biosciences (stock number 1638) were bred. PCR genotyping was conducted with human tau transgene (forward 5'-ACTTTGAACCAGGATGGCTGAGCCC-3', reverse 5'-CTGTGCATGG CTGTCCCTACCTT-3'). At 20 weeks of age, ouabain at a dose of 1.5 μg/kg or vehicle (saline) was administered by intraperitoneal injection for 6 weeks (3 times a week). All mice were sacrificed after the behavior test at a final age of 26 weeks. Body weight was measured once a week prior to the treatment. All the mice used in this study had a C57BL6 background. Animals were bred at the Laboratory Animal Facility in the Asan Institute for Life Sciences under specific pathogen-free conditions and maintained at a constant ambient temperature (22 ± 1°C) with a 12-h light-dark cycle. Animals were housed 3-5 per cage with ad libitum access to food and water. Littermates were used in all experiments. All experiments were designed to minimize the number of animals used, and all procedures were carried out in accordance with the Institute of Laboratory Animal Resources (ILAR) Guide for the Care and Use of Laboratory Animals. This study was reviewed and approved by the Institutional Animal Care and Use Committee of the Asan Institute for Life Science (approval number. 2015-02-093).

2. 14. 2. Y maze test

The Y maze test was performed as described in previous studies (42). Specifically, the Y maze was made of polyvinylidene and had 3 arms, and each arm (8(width) × 35(length) × 15(high) cm) had an angle of 120°. The 3 arms included a starting arm (always open), where

the mouse began to explore; a novel arm, which was blocked in the first trial but held open in the second trial; and a third arm (always open). In the experiment, the starting arm and the third arm were randomly designed to avoid spatial memory errors. The Y-maze test was performed by dividing the 2 tests by the inter-test interval (ITI). In the first trial, the mouse searches for 2 arms for 5 min, except for the blocked novel arm. After 4 h, a second trial was performed. In the second trial, the mice were free to enter all 3 arms for 5 min, and were placed in the same labyrinth position as in the first experiment. The spatial recognition memory was analyzed by the number of alternation and the spent of time in new arm region (learned behavior). Each arm of the Y maze was rinsed with 70% ethanol between trials.

2. 15. Statistical analysis

All details of sample sizes and reproducibility are shown in the figure legends. Data are presented as means ± standard error of the mean (SEM), based on 3 independent experiments. The data were analyzed using one-way analysis of variance (ANOVA), followed by the Tukey post-hoc test.

3. Results

3. 1. Two-step screening assay for protective effect against OA-induced neurodegeneration and for TFEB activation

Two targeted screening systems, the protection from neurotoxicity of tau and the stimulation of the autophagy-lysosomal pathway through activation of TFEB, were screened using the LOPAC1280 library of pharmacologically relevant compounds. This library is biologically annotated collection of inhibitors, receptor ligands, pharma-developed tools, and approved drugs impacts most signaling pathways and covers all major drug target classes.

To confirm compounds of neuro-protective effect, the ATP assay was used in OA-induced neurodegeneration model (Fig. 1a). Using high throughput screening of LOPAC^{1280} library, I considered compounds with a cut-off value (Z-score) of ≥ 4 as potential hits (Fig. 2a); primary hits, six out of 1,280 compounds, were identified as putative candidates with the ability to improve neuron survival. To confirm compounds of autophagy-lysosome activity effect, the effect on TFEB activity was tested using the LOPAC^{1280} library (Fig. 1b). Transcriptional competence of TFEB is modulated by physical compartmentalization in the cytosol versus the nucleus. Therefore, TFEB translocation to nucleus was analyzed using high-content screening for compounds in GFP-TFEB transfected Hela cells. Seven active compounds with a cut-off value of ≥ 2 as potential hits showed persistent TFEB nuclear localization (cut-off> 2; Fig 2b). As a result, the ouabain, which has significant activity in OA-induced neuroprotection and TFEB activation, was identified (Fig. 1c and 2c).

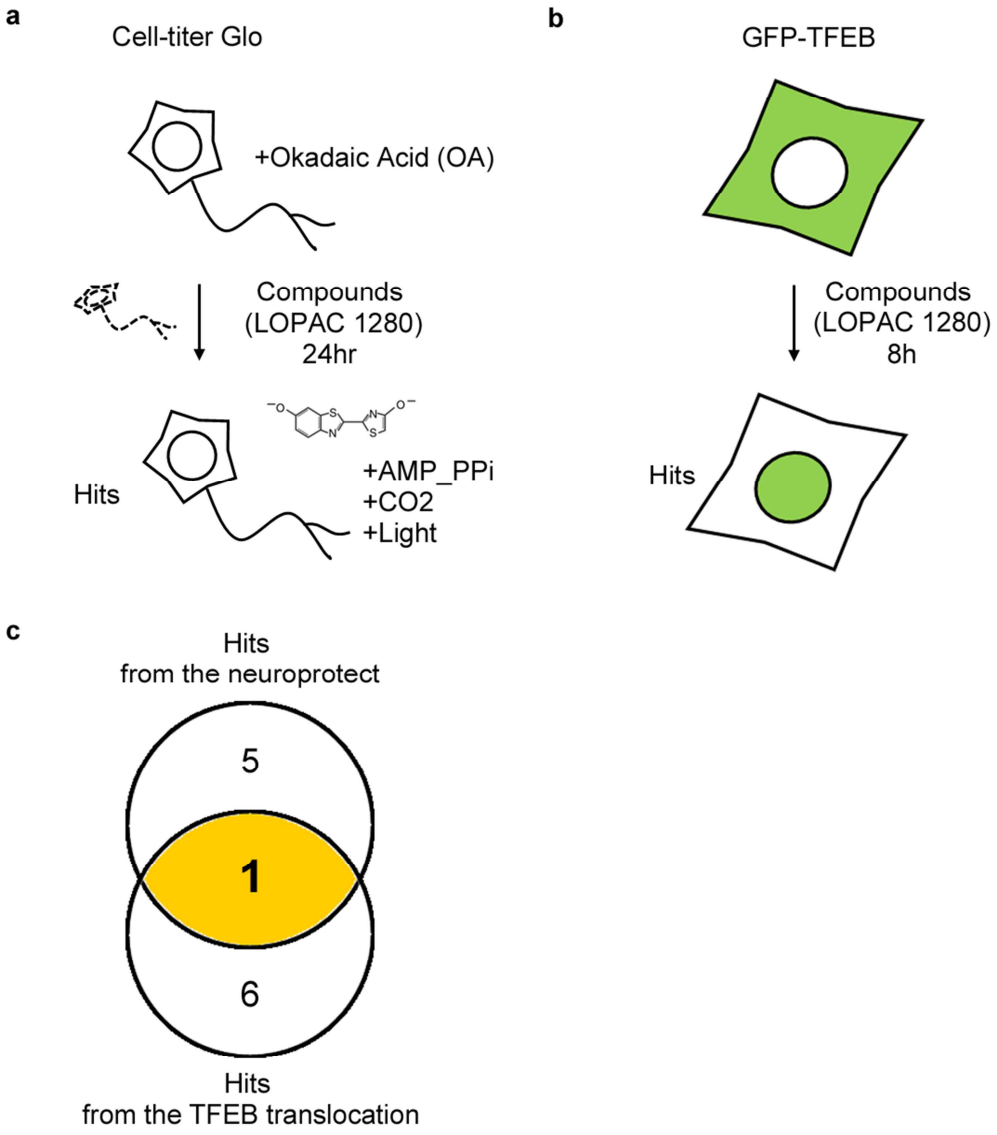

Figure 1. A cell-based screen workflow. Schematic of workflow used to screen and validate neuroprotective (**a**) and TFEB translocating (**b**) drugs. (**c**) Schematic showing overlapping compounds among the top hit lists from the 2 screens.

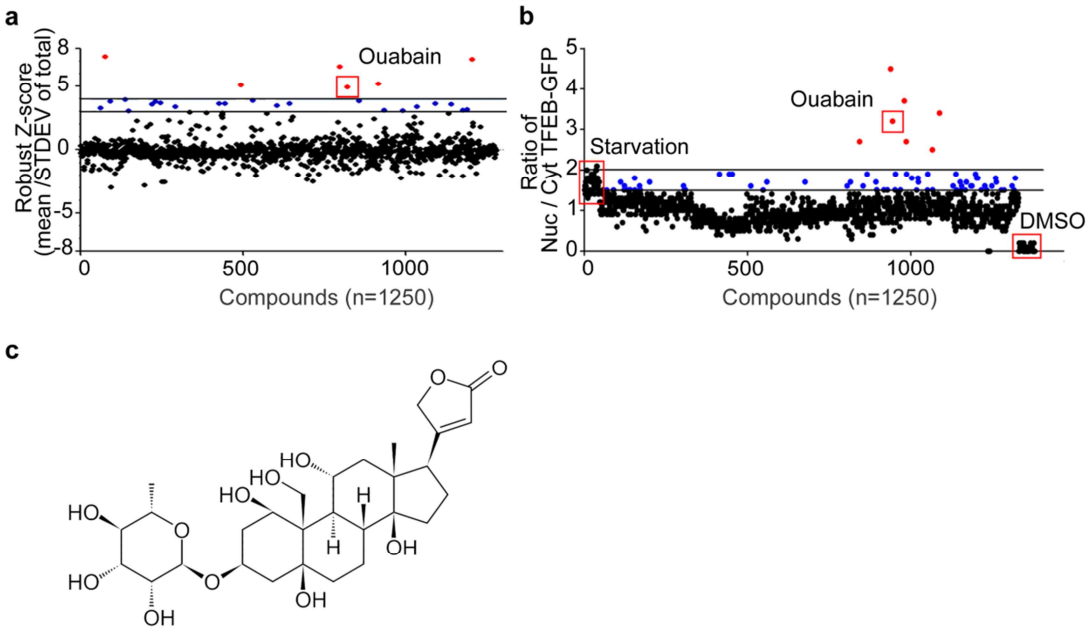

Figure 2. Ouabain improves cellular content of ATP and induces TFEB nuclear translocation. (**a**) Robust Z score of >4 identified 6 compounds from the cellular ATP activity screen. (**b**) The plot of the NucGFP/Cyt-GFP ratio of two of seven identified compounds from TFEB screen. (**c**) The chemical structures of ouabain.

3. 2. Ouabain protects against OA-induced neuronal damage

To confirm the neuroprotective effects of ouabain, the compound selected in the primary screening, the assay examined about neuronal cytotoxicity and viability using ATP, LDH and MTT assays. ATP reduction was recovered in the presence of ouabain dose-dependently (Fig. 3a). In particular, ATP levels increased more than 2-fold in the presence of 5 μM ouabain. The amount of LDH released into media was measured for the mechanism of cytotoxicity. In the cell toxicity assay, exposure to ouabain increased neuroprotection by 30% compared to OA only (Fig. 3b). This suggests that ouabain protects cell membrane damage caused by OA. A colony formation assay was performed to more accurately determine the effect of ouabain on cytotoxicity. The neuronal viability was fully restored in the presence of ouabain (Fig. 3c) as compared to the OA-only condition. The length of MAP2 stained neurite was measured and analyzed on an average of 200 cells. OA-treated neurons had a 30% reduction in neurite length compared to normal, while ouabain treatment remained up to 80% in neurite length (Fig. 3d; MAP2 immunofluorescence, red). These data suggest that ouabain effectively prevented neuronal damage in OA-treated neurodegeneration model.

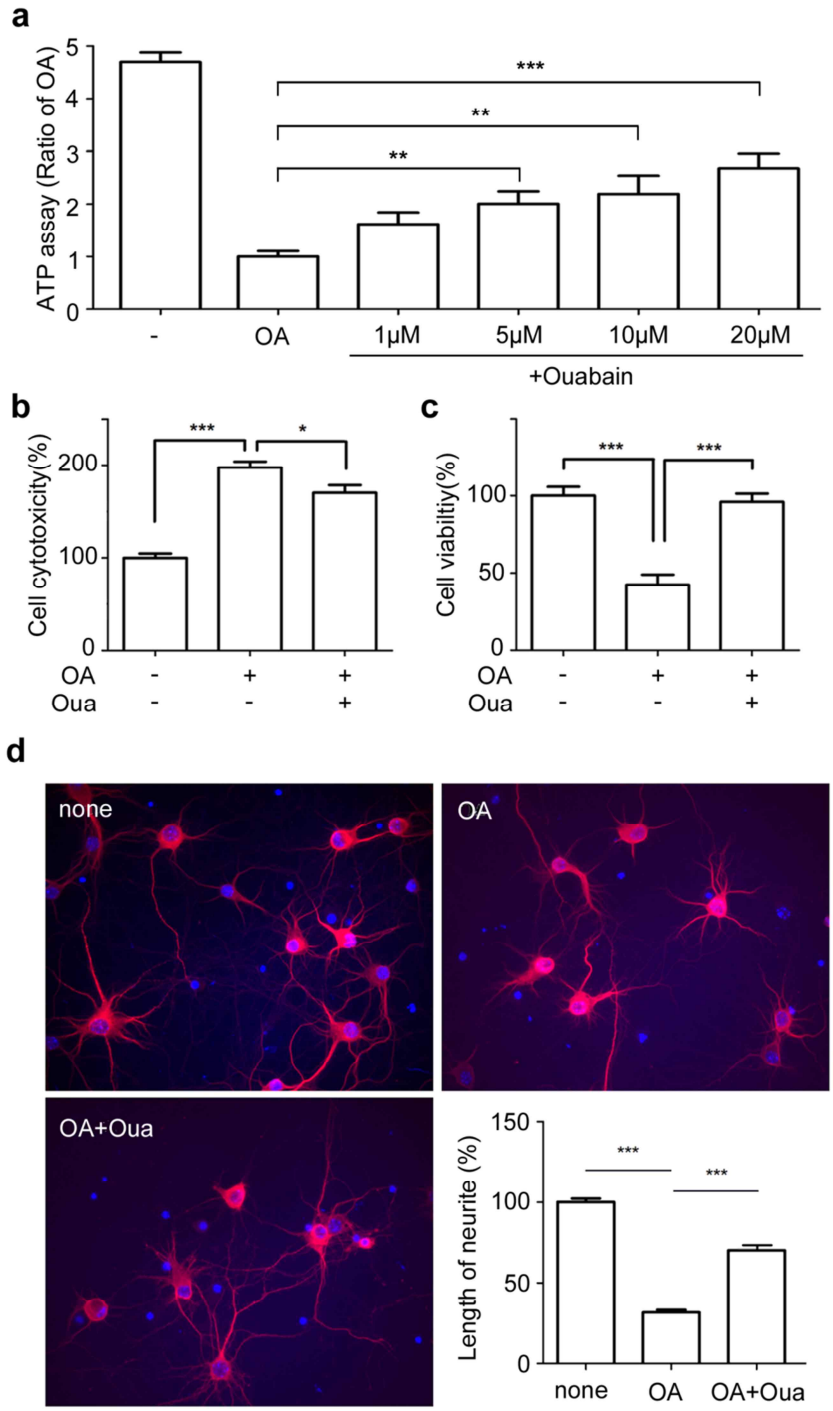

Figure 3. Ouabain exhibits neuroprotective activity against OA-induced neurodegeneration in vitro. (**a**) Mouse primary cortical neurons (DIV 10) were incubated with 10 nM OA for 24h pre-treated with the indicated concentration of ouabain. The graph

represents the ratio of OA. (mean ± s.d. for n = 3 independent experiments, **p < 0.01, and ***p < 0.001 by one-way ANOVA, the Tukey post-hoc test). (**b-d**) Primary neurons were treated with 10 nM OA for 24 h, following pretreatment with 0.5 μM ouabain. Cell cytotoxicity and viability were examined using LDH in **b** and MTT in **c** assays, respectively. (mean ± s.d. for n = 3 independent experiments, *p < 0.05, and ***p < 0.001 by one-way ANOVA, the Tukey post-hoc test). (**d**) In immunofluorescence microscopic images of neurons (MAP2-red), neurite length was analyzed under different culture conditions to show outgrowth recovery after treatment with ouabain. Scale bar, 20 μm. (mean ± s.d. for n = 200 neurons per group from 3 independent experiments, ***p < 0.001 by one-way ANOVA, the Tukey post-hoc test).

3. 3. TFEB activation and autophagy gene regulation

In normal conditions, phosphorylated TFEB is located in the cytoplasm, whereas in some conditions, such as starvation, TFEB is dephosphorylated and translocated from the cytosol to the nucleus (29). In the presence of ouabain, TFEB was dephosphorylated and active in HeLa cells (Figs. 4a, b) and neurons (Figs. 4c, d). The molecular size of nuclear TFEB was slightly lower than cytoplasmic TFEB (see Figs. 4a and c, arrowhead), indicating that TFEB was dephosphorylated and active. In addition, I observed TFEB translocation from ouabain-treated cytoplasm to nucleus (Fig. 4b and d) through fluorescence imaging of GFP-TFEB after staining with Hoechst, a nuclear marker and phalloidin, an actin cytoskeleton marker in HeLa cells and neurons.

Dephosphorylated, active TFEB induces the autophagy-lysosome pathway by acting, as a transcription factor to increase the expression of αutophagy-1ysosome related proteins such as p62/sequestosome (SQSTM) 1, LAMP1 and LC3B (43, 44). In Hela cells (Fig.5a) and neurons (Fig.5d), ouabain significantly increased the level of autophagy-lysosome related proteins, LAMP1 and LC3B. These results were further supported by fluorescence analysis using Lysotracker (Figs. 5b, e) and LC3B (Figs. 5c, f). Lysotracker-Red selectively stains the acidic lysosomal organelles. OA inhibits autophagy induced by metabolic stress resulting in accumulation of autophagosomes in neurons (45). The level of Lamp1 and LC3B investigated under OA alone or ouabain, which confirmed a pattern of increase (Figs. 5g-i). LC3BII showed a 2-fold increase compared to OA-alone (Fig. 5i). These results indicate that ouabain can promote biogenesis of lysosome and activation of autophagy-lysosomal system via augmenting TFEB activity.

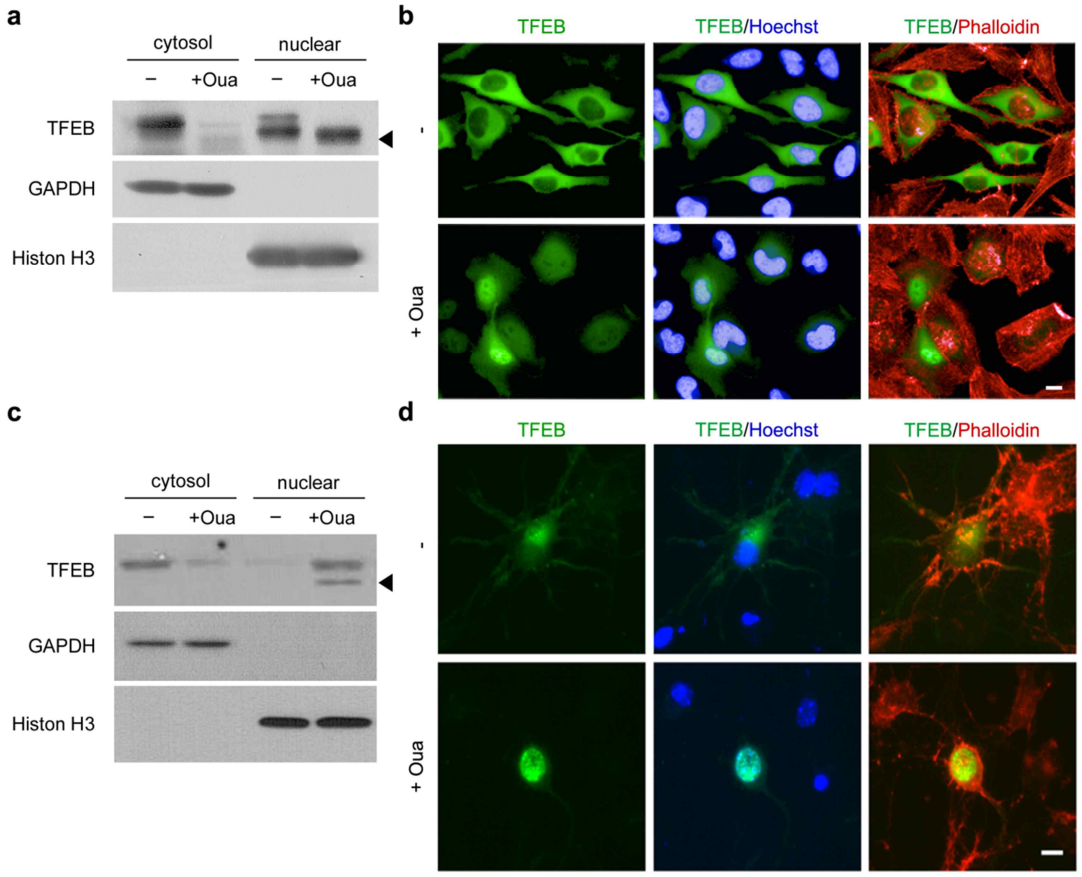

Figure 4. Ouabain induces cytosol-to-nucleus translocation of TFEB. HeLa cells (**a-b**) and mouse primary cortical neurons (**c-d**) were incubated with 0.5 μM ouabain for 8 h. (**a, c**) The cytosol and nuclear fractions were assessed for TFEB translocation by ouabain. Western blots show distribution of TFEB translocation from cytosol to nucleus after ouabain treatment in HeLa (with TFEB-antibody for human) and neurons (with TFEB-antibody for human and mouse). Arrow head shows the dephosphorylated TFEB. The blot was probed with antibodies to histone H3, a marker for the nuclear fraction, and GAPDH, a marker for the cytosol fraction. (**b, d**) The fluorescence images show localization of GFP-TFEB after ouabain treatment in HeLa and neurons. Scale bar, 10 μm.

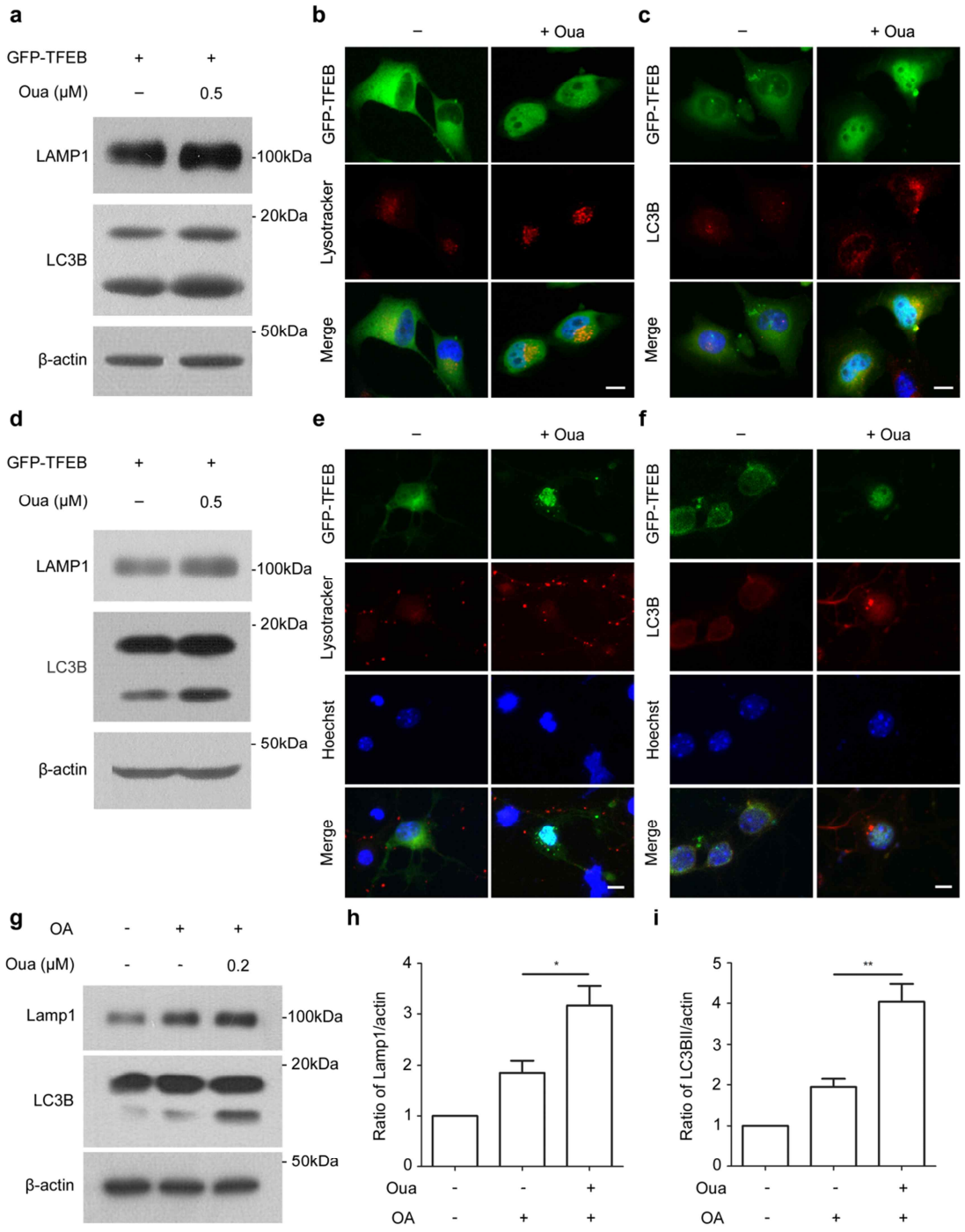

Figure 5. Ouabain up-regulates autophagy–lysosome clearance system. GFP-TFEB in HeLa cells (**a-c**) and primary cortical neurons (**d-f**) were incubated with or without 0.5 μM ouabain for 8 h. (**a, d**) Western blot analysis of LAMP1 and LC3B, autophagy related

proteins, in HeLa (**a**) and neurons (**d**). (**b, e**) The fluorescence images showed punctate pattern of Lyso-tracker, a marker of autophago-lysosome in HeLa (**b**) and neurons (**e**). Scale bar, 10 μm. (**c, f**) The immunofluorescence images showed punctate of LC3B, a marker of autophagy-related protein, observed in Hela (**c**) and neurons (**f**). Scale bar, 10 μm. (**g-i**) Primary cortical neurons (DIV 10) were incubated in 10nM OA or with 0.2μM ouabain for 8h. (**g**) Western blot analysis of LAMP1 and LC3B in OA or with ouabain. (**h, i**) Quantification of Lamp1 (**h**) and LC3BⅡ (**i**) relative to treated vehicle. (mean ± s.d. for n = 3 independent experiments, *$p < 0.05$ and **$p < 0.01$ by one-way ANOVA, the Tukey post-hoc test).

3. 4. Phosphorylated tau is reduced through the autophagy-lysosomal pathway

Recent studies of the tauopathy mouse model showed that pathological tau species are effectively reduced via TFEB activation and downstream autophagy pathway (26). To confirm that ouabain regulates phosphorylated tau (p-tau) via TFEB activation, the experiments were conducted in GFP-TauP301S overexpressed SH-SY5Y (Fig. 6a) and primary cortical neurons (DIV6; Fig. 6d). In both SH-SY5Y and neurons, the p-tau species (Ser199/202 and Ser396 region) significantly reduced in ouabain treatment (Figs. 6b, c and Figs. 6e, f). Intracellular abnormal proteins are typically degraded through the proteasome or autophagy-lysosome (46-48).

To study the relationship between phosphorylated tau reduction and intracellular clearance system, the inhibitors, MG 132 (a proteasomal protease inhibitor) and bafilomycin A1 (the lysosomal decomposition inhibitor), were processed and confirmed p-tau levels in blots. Indeed, bafilomycin A1 blocked ouabain-induced tau clearance (Thr231; AT180 and Ser396 region), whereas MG 132 had no effect on the p-tau level (Figs. 6g-i). This result shows that ouabain reduces p-tau through the autophagy-lysosome pathway, not the ubiquitin-proteasome pathway.

To evaluate these data in another physiological condition, a similar experiment was performed in the OA-induced neurodegeneration model (Fig. 6j). The p-tau species (Thr 231; AT 180, Ser 199/202 and Ser 396 region) in OA-treated conditions were significantly decreased by ouabain (Figs. 6k-m).

Because the mechanistic target of rapamycin complex 1 (mTORC1) is a negative regulator of autophagy (49, 50), western blots were analyzed in phosphorylation of p70S6K and 4EBP1, downstream proteins of mTORC1. The phosphorylated 4EBP1 and p70S6 kinase

were significantly decreased in a time- and dose-dependent manner following treatment with ouabain (Figs. 7a-d). Upon exposure to OA, phosphorylation of mTOR (Ser2448) and its substrate, p70S6K, are increased (51). In OA-treated neurons, blots also were analyzed in downstream proteins of mTORC1. In the presence of ouabain, there was a significant decrease in phosphorylated mTOR and p70S6K (Figs. 7e-g). These results reveal that ouabain induces autophagy by dephosphorylation and activation of TFEB, whose action is dependent on mTORC1 inhibition.

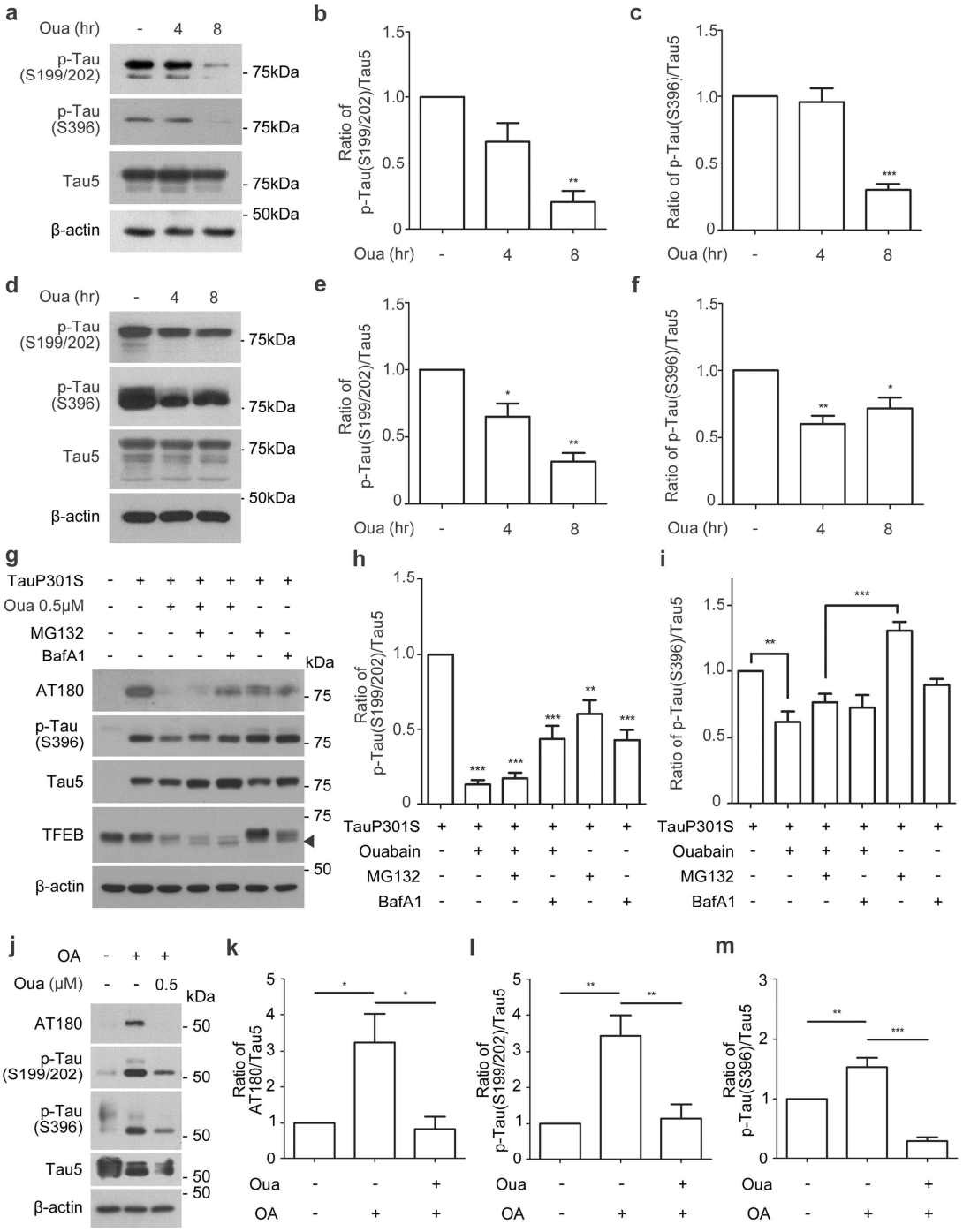

Figure 6. Ouabain decreases phosphorylated tau via autophagy–lysosome pathway. GFP-TauP301S transfected SH-SY5Y cells (**a-c**) and mouse primary cortical neurons (**d-e**) were treated with 0.5μM ouabain. (**a** and **d**) Western blot analysis phosphorylated tau at

Ser199/202 and Ser396 and total tau (Tau5) after ouabain treatment in SH-SY5Yand neurons. (**b**, **c**, **e** and **f**) Quantification of phosphorylated tau (Ser199/202 in **b** and **e**, Ser396 in **c** and **f**) relative to treated vehicle. (mean ± s.d. for n = 3 independent experiments, *p < 0.05, **p < 0.01 and ***p < 0.001 by one-way ANOVA, the Tukey post-hoc test). (**g-j**) Primary cortical neurons (DIV 10) were incubated with 10 nM OA or 0.2μM ouabain for 8 h. (**g**) Western blot analysis tau phosphorylated at Thr231 (AT180), Ser199/202 and Ser396, and total tau (Tau5) after treatment in neurons. (**h-j**) Quantification of phosphorylated tau (Thr231 in **h**, Ser199/202 in **i** and Ser396 in **j**) relative to treated vehicle. (mean ± s.d. for n = 3 independent experiments, *p < 0.05, **p < 0.01 and ***p < 0.001 by one-way ANOVA, the Tukey post-hoc test). (**k-m**) Primary cortical neurons (DIV 5) were transfected with GFP-TauP301S, and pre-treated with vehicle or 0.5 μM ouabain (8 h) before treated with 5 μM MG132 (1 h) or 25 nM bafilomycin A1 (4 h). (**k**) Western blot analysis tau phosphorylated at Thr231 (AT180) and Ser396, total tau (Tau5), and TFEB. Arrowhead indicates the dephosphorylated TFEB. (**l** and **m**) Quantification of phosphorylated tau (Thr231; AT180 in **l**, Ser396 in **m**) relative to treated vehicle. (mean ± s.d. for n = 3 independent experiments, **p < 0.01 and ***p < 0.001 by one-way ANOVA, the Tukey post-hoc test).

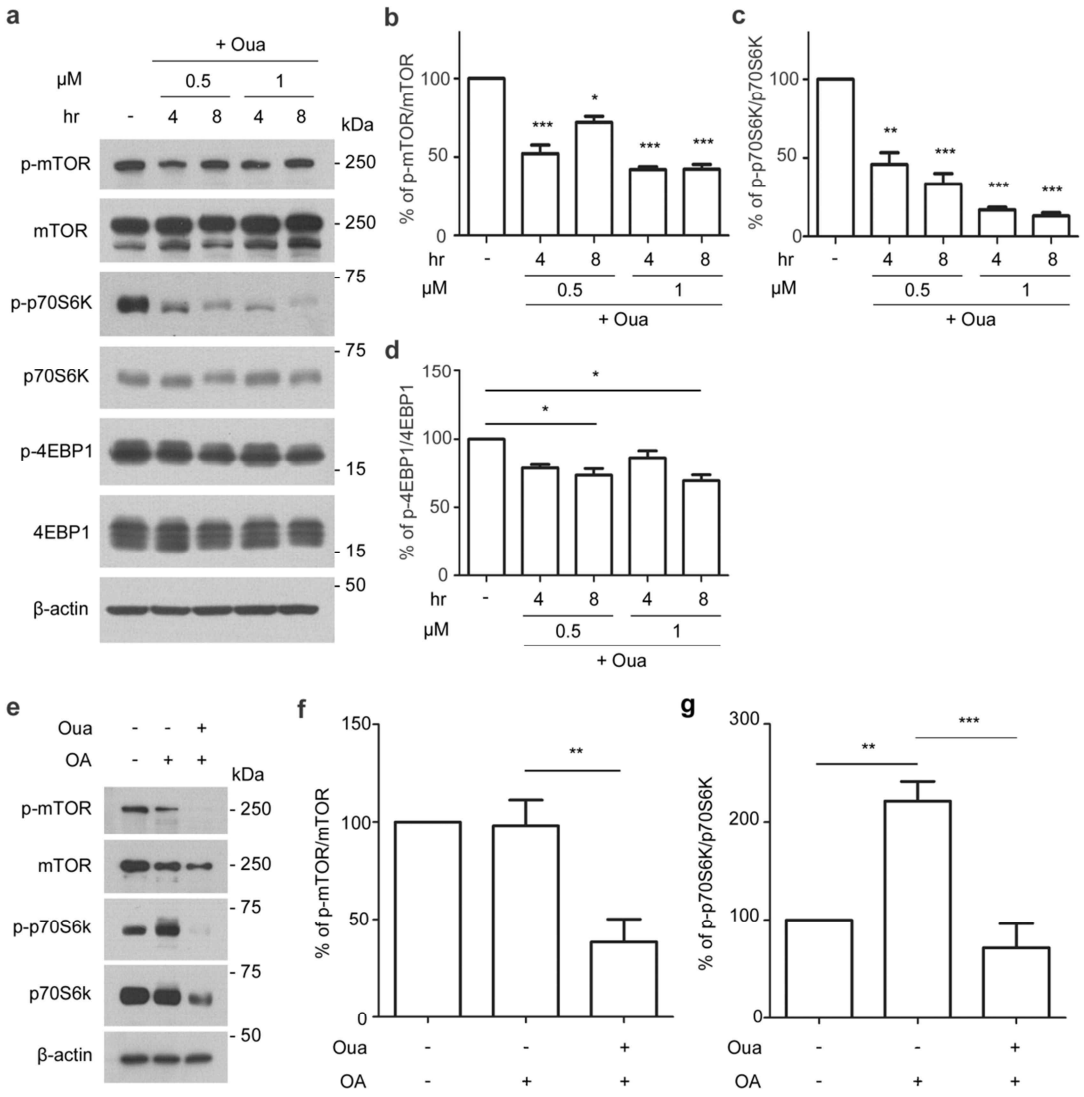

Figure 7. Ouabain inhibits mTOR. (**a-d**) GFP-TauP301S SH-SY5Y cells were treated with vehicle or ouabain (0.5 μM). (**a**) Western blot analysis of mTOR, p70S6K, and 4EBP1 phosphorylation after ouabain treatment. (**b-d**) Quantification of phosphorylated mTOR, p70S6K, and 4EBP1 relative to treated vehicle. (mean ± s.d. for n = 3 independent experiments, *p < 0.05, **p < 0.01 and ***p < 0.001 by one-way ANOVA, the Tukey post-hoc test). (**e-g**) Mouse primary cortical neurons (DIV 10) were treated by 10 nM OA with or without ouabain (0.2 μM) for 8 h. (**e**) Western blot analysis of mTOR and p70S6K

phosphorylation after treatment in neurons. (**f, g**) Quantification of phosphorylated mTOR and p70S6K relative to treated vehicle. (mean ± s.d. for n = 3 independent experiments, **p < 0.01 and ***p < 0.001 by one-way ANOVA, the Tukey post-hoc test).

3. 5. Ouabain treatment decreases p-tau and neurodegeneration in a *Drosophila* tau model

In order to address the effects of ouabain *in vivo*, a *D. melanogaster* model of tauopathy in which human tau were used, which expressed through the glass multiple reporter promoter (gmr-Gal4 > tau). This produces a "rough-eye" phenotype with disordered and fused ommatidia (52). The ouabain were administered in food during the larval period at a concentration of 2 μM and 20 μM in three double-blind rounds and then the eye phenotype was assessed in adults (Fig. 8a). This allowed to directly evaluation responses in eye-phenotype and ommatidia. The average lifespan of all the ouabain-uptake flies was no different from solvent-uptake flies, indicating that the ouabain did not cause generalized toxicity (Fig. 8b). After ouabain ingestion, gmr-Gal4 > tau-2N4R *Drosophila* clearly exhibited well-organized ommatidia compare to control (Fig. 9a) and decreased phosphorylated tau (Fig. 9b), confirming the protective effect against tau overexpression in fruit flies. A microphthalmia-associated transcription factor (dMitf) is the only homolog of TFE3 and human TFEB in fruit flies (53). I investigated whether dMitf could be involved in the reduction of p-tau and improvement of the rough-eye phenotype. Tau2N4R-expressing flies with knockdown of dMitf (dMitfKD), exhibited abolished ouabain-induced improvement in their ommatidia (Fig. 9c), and the rough-eye phenotype was observed in all progeny. Protein levels also did not find significant changes in the amount of p-tau by with or without ouabain in this model (Fig. 9d). These results suggest that Mitf (also known as TFEB), is necessary for ouabain-induced p-tau reduction in *D. melanogaster*.

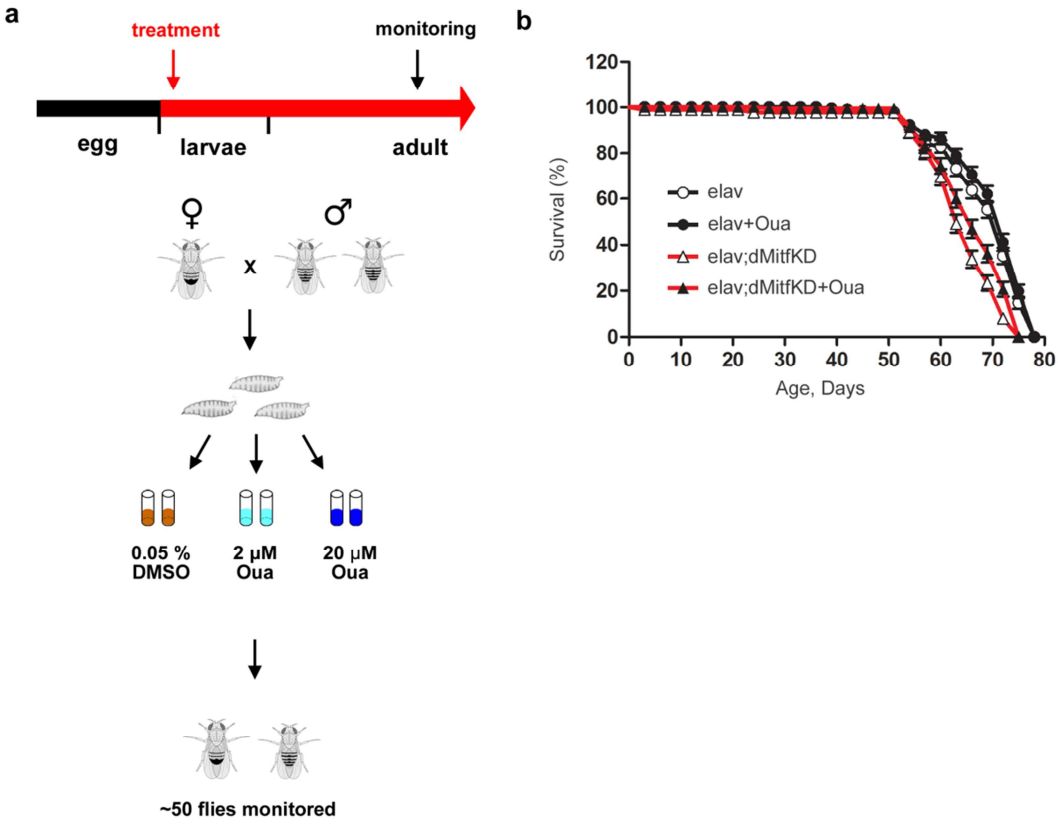

Figure 8. Effect of ouabain on the transgenic flies. (**a**) Schematic of the eye phenotype assay. (**b**) No significant lifespan difference was observed according to uptake of ouabain-treated food between elav or elav;dMitfKD flies. Elav;dMitfKD flies tended to have a shorter lifespan than controls, but no difference attributed to ouabain was observed. n = 200 per group.

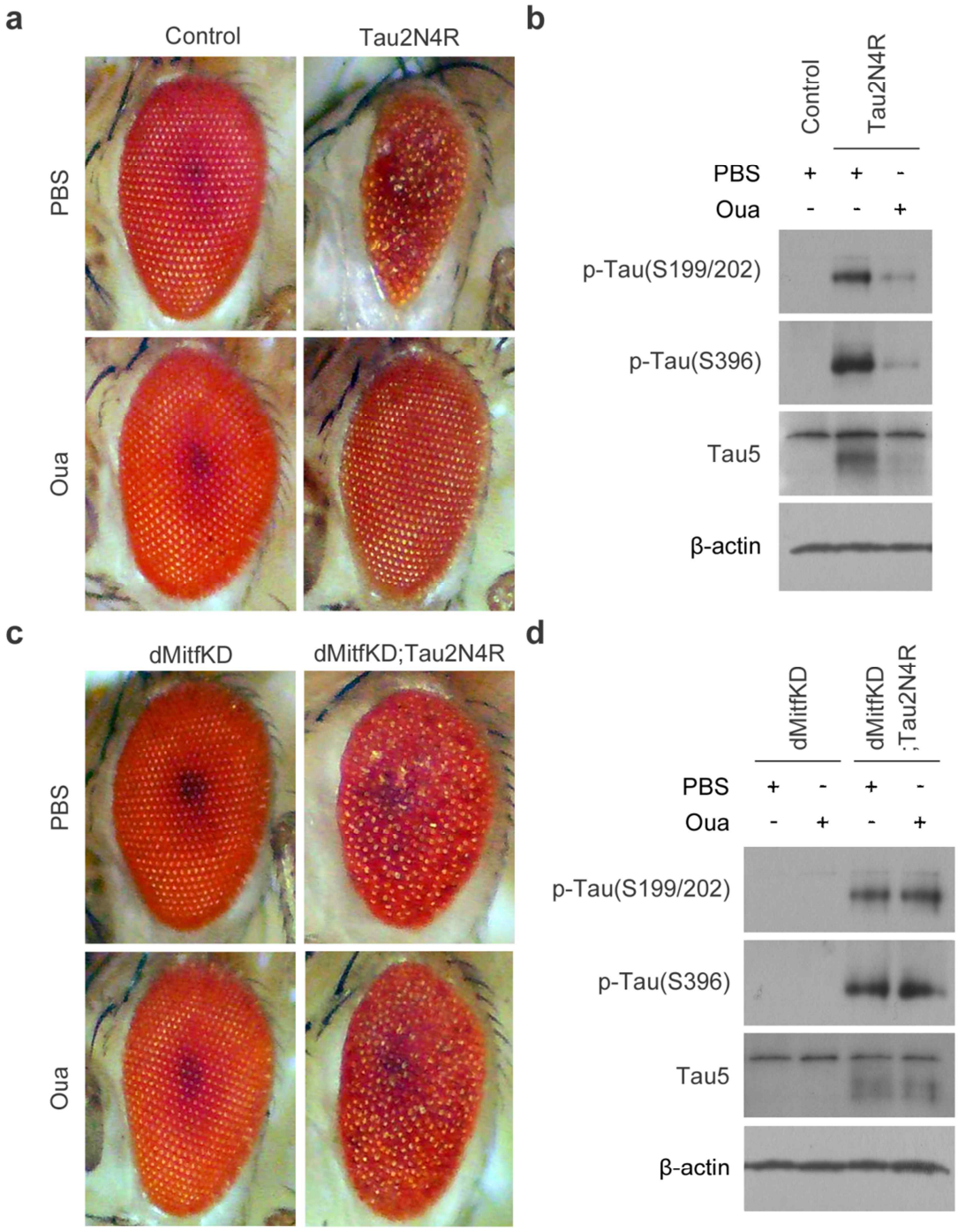

Figure 9. Ouabain improves the gmr<tau phenotype and is related to dMitf/TFEB expression in *Drosophila*. (**a**) The eyes of adult flies overexpressing human tau 2N4R, under the control of the eye-specific gmr-Gal4 driver, expressed abnormal surface and

condensation of the size (upper right). This eye defect was effectively rescued by feeding with 2 μM of ouabain (bottom right). n = 50 per group. (**b**) Western blot analysis of tau phosphorylated at Ser199/202 and Ser396, and total tau (Tau5). (**c**) The eyes of dMitfKD;Tau2N4R adult flies, and of control flies bearing only dMitfKD. The eyes of dMitfKD;Tau2N4R adult flies expressed abnormal surface (upper right). This eye defect was not changed by feeding with 2 μM of ouabain (bottom right). n = 50 per group. (**d**) Western blot showing distribution of tau phosphorylated at Ser199/202 and Ser396, and total tau (Tau5).

3. 6. Ouabain ameliorates the memory deficit in TauP301L mice and reduces the tau level

To test whether ouabain has therapeutic effects on memory impairment of AD, the behavior test was performed in JNPL3 transgenic mice, a tau-P301L tauopathy model. These mice present an adjustable level of human tau with a P301L mutation and are associated with age-dependent pathology, neurodegeneration, and gradual onset of memory deficits (54), similar to those seen in AD, the most common tauopathy. TauP301L mice exhibit age-related spatial memory deficits due to neuronal loss caused by increased accumulation of hyperphosphorylated tau and NFTs (54, 55). To confirm that ouabain did not have an overt harmful effect, body weight and locomotor activity were assessed. There was no significant difference in body weight in any of the groups between the initial stage and the end of the experiment (Fig. 10b). An anxiety-related measure, the total distance in open field, was similar between WT and TauP301L groups in 6-month-old mice (Fig. 10c). Treatment with 1.5 μg/kg ouabain had no significant effect on WT or TauP301L mice. These results suggest that ouabain treatment is not toxic and did not cause any change in the search behavior or anxiety level of the mice used in the experiment. To determine whether ouabain modifies memory deficits in Tau mice, a Y-maze test was performed (Fig. 11a) in 20-weeks–old TauP301L mice and wild-type littermates with or without ouabain injection. Spontaneous alternation in the Y-maze, an index of short-term spatial working memory in mice, was evaluated in TauP301L and wild-type (WT) strains, and no significant differences in mouse activity in the new arm were observed between the groups (Fig. 11b). However, the time in new arm was significantly improved in TauP301L mice injected with ouabain compared with TauP301L mice (Fig. 11c). Time-resolution analysis in the new space showed a 40% reduction in tau mice compared to WT mice (with or without ouabain), significantly improved behavior in ouabain-injected TauP301L mice, restoring memory to WT-like levels

(Fig. 11c).

Western blot analysis using antibodies against p-tau (S199/202 and S396) and total tau (Tau 5) at the end of behavior tests showed that intraperitoneal ouabain injection markedly reduced p-tau species in both the cortex (Fig. 11d) and hippocampus (Fig. 11e) of TauP301L mice. In the cortex of TauP301L mice, the amount of p-tau (S199 / 202 and S396 region) versus total tau was reduced to half of the initial level after ouabain treatment, whereas WT mice showed no change in the amount of p-tau even after ouabain treatment (Figs. 11f, g). In the hippocampus of TauP301L mice, the amount of pS199/202 tau versus total tau reduced to half of the initial level after ouabain treatment (Fig. 11h). For p-tau (S396), the value of the change was not significant (Fig. 11i). These results suggest that ouabain decreases p-tau and improves behavioral disturbances caused by hyper-phosphorylated tau.

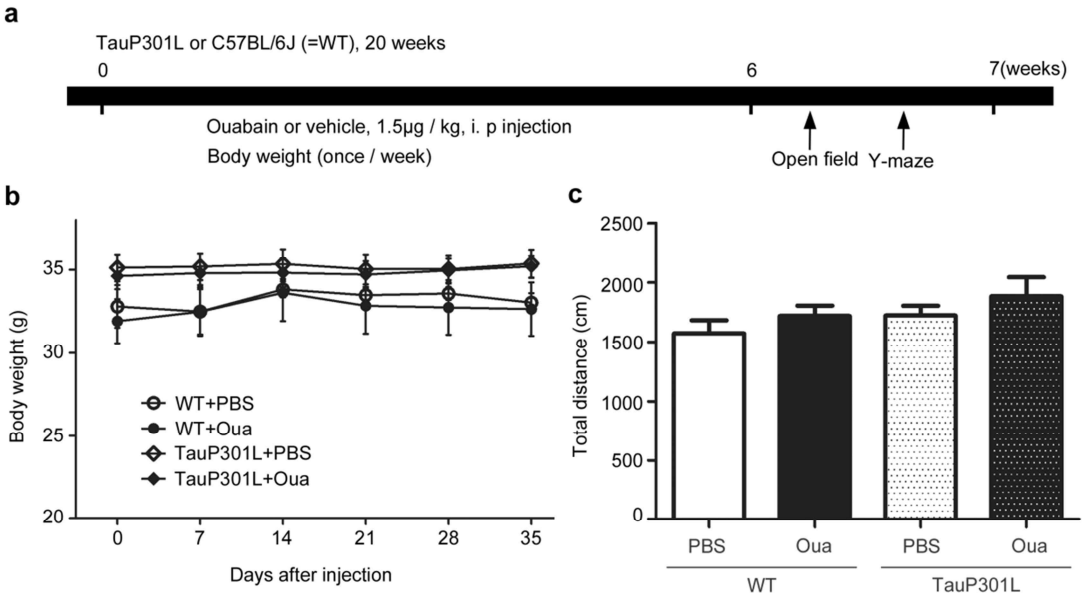

Figure 10. Effects of ouabain on body weight and total distance. (**a**) Experimental paradigm for the drug injection and behavioral testing. Mouse were injected (i.p.) for the 6 weeks post-injury with either 1.5 μg/kg ouabain or vehicle. (**b**) Body weight following intraperitoneal injection of ouabain or PBS. (**c**) Quantification of the total distance by animals from open field areas in treated ouabain or not. n=4, each of WT groups and n=10, each of TauP301L groups.

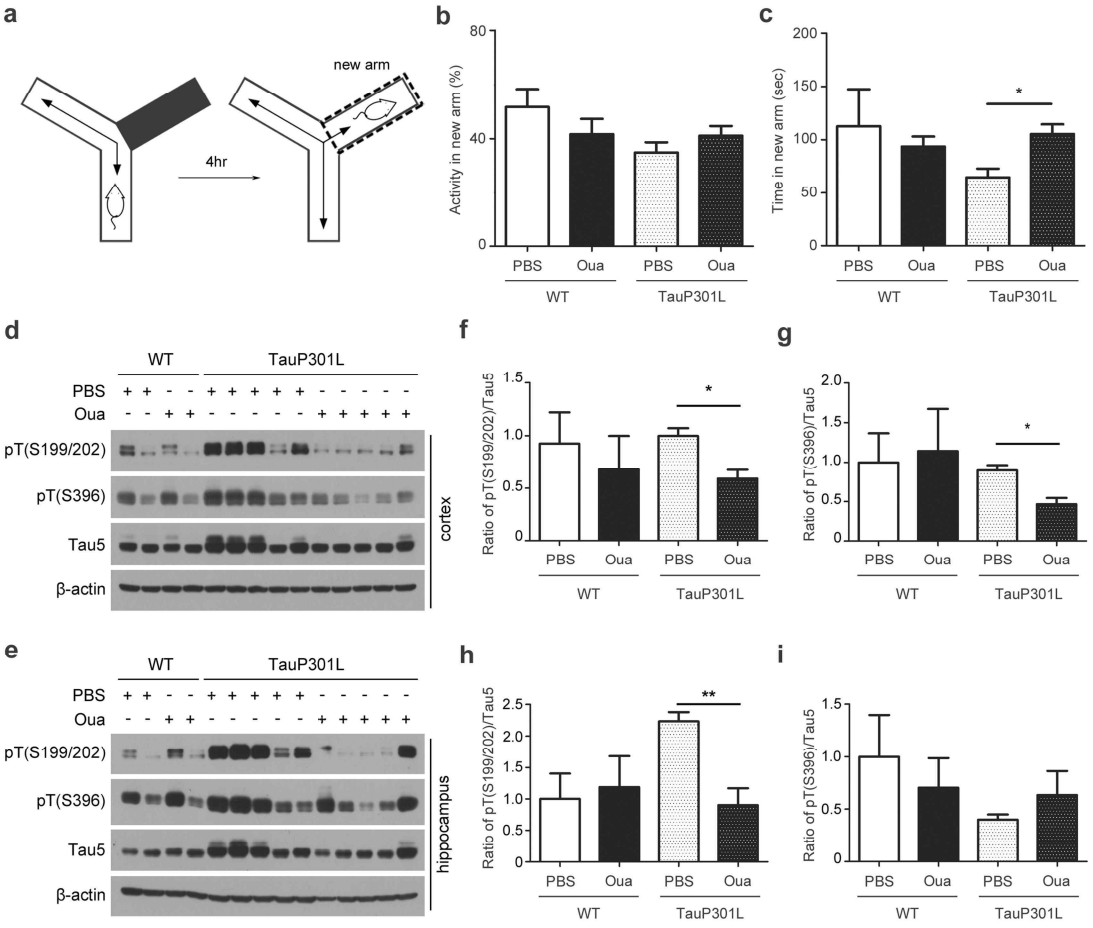

Figure 11. Effect of ouabain in TauP301L mice with induced memory impairment and elevated tau level. (**a**) Schematic diagram of the Y maze apparatus. (**b**) The number of alternation in new arm region by control and TauP301L mice treated with vehicle or 1.5 μg/kg ouabain. (**c**) The spent of time in new arm region by control and TauP301L mice with vehicle or 1.5 μg/kg ouabain. (**d-e**) The cortex (**d**) and hippocampus (**e**) of wild-type and TauP301L mice injected with vehicle or ouabain were homogenized for immuno-blot. Western blot analysis of tau phosphorylated at Ser199/202 and Ser396, and total tau (Tau5). Quantification of phosphorylated tau at Ser199/202 and Ser396 normalized with Tau5 in cortex (**f, g**) and hippocampus (**h, i**). n=4, each of WT groups and n=10, each of TauP301L

groups. (mean ± s.d. for n = 3 independent experiments, *p < 0.05 and **p < 0.01 by one-way ANOVA, the Tukey post-hoc test).

4. Discussion

In this study, ouabain discovered as a common-hit compound, both among the neuroprotective compounds and in the TFEB activator screening. Ouabain treatment resulted in protective effects in both the *in vitro* OA-induced neurodegeneration model and the *in vivo* tau transgenic fly and P301L mouse models.

Ouabain is well known as a plant-derived toxic substance that was used as an arrow poison. However, in lower doses, it can be used medically to treat hypotension and arrhythmias (56). Intravenous ouabain has a long history in the treatment of heart failure in France and Germany (57). Endogenous ouabain was discovered in the human blood as a regulatory hormone (58, 59). In a rat model of pregnancy-induced hypertension, ouabain reduced mean arterial pressure without any adverse effects on pups, suggesting the potential therapeutic application in preeclampsia (60). Ouabain may also play a role in suppressing cancer metastasis via integrin regulation (61). Ouabain pretreatment induced concentration- and time-dependent RNA/DNA synthesis and overexpression of many stress-induced signals, including the production of mortalin (heat shock protein 70), c-Fos, and c-Jun proteins. A neuroprotective effect by ouabain at low concentrations was also reported in traumatic brain injury (62). I also observed ouabain's protective effects in tau transgenic mice at low concentrations with no overt side effects (Figs. 10 and 11).

This study reveals that ouabain decreases phosphorylated tau accumulation and tau pathology (Figs. 6-11) via TFEB-induced autophagy activation (Figs. 2, 4, and 5). Ouabain and other cardiac glycosides have been reported to activate autophagy in tumor cells (63-66), which further accords with our findings. Ouabain's *in vivo* protective effect is dependent upon TFEB, as demonstrated by our findings that the tau-induced rough-eye phenotype was improved by ouabain, but was abolished by knock-down of *Drosophila* TFEB (Fig. 9). The

effect of ouabain on tau reduction is also dependent upon TFEB-induced autophagy; the inhibition of lysosomal degradation with bafilomycin-A1 abolished the tau reduction effect (Figs. 6f and g). These results suggest that ouabain, a Na/K-ATPase inhibitor, can be used therapeutically in AD or tauopathy, inducing tau reduction through the autophagy-lysosomal pathway enhanced by the activation of TFEB.

The activity of TFEB is regulated by mTOR and calcineurin, where mTOR phosphorylates TFEB at S142 and S211 to sequester it in the cytosol, while calcineurin dephosphorylates TFEB to move it to the nucleus (50, 67, 68). The mTOR pathway is involved in cellular processes and pathways affected by the Na/K-ATPase effect (69, 70). Ouabain inhibits mTOR in neuronal cells (Fig. 7), thereby contributing to the activation of TFEB. Na/K-ATPase, by binding to cardiotonic steroids such as ouabain, induces multiple cell signaling pathways and promotes autophagy (63). It was also recently reported that digoxin inhibits Na/K-ATPase, increasing the cytosolic Ca^{2+} level, which activates calcineurin and inhibits mTOR, leading to TFEB dephosphorylation and activation (38). Indeed, pharmacologic intervention directed at upstream targets of TFEB activation such as mTORC1 inhibitors (71) and AMPK activators (72) or digoxin (38), a Na/K-ATPase inhibitor, has already demonstrated significant potential for mitigating metabolic abnormalities and even prolonging lifespan. Nevertheless, ouabain has a narrow therapeutic range due to cardiovascular risk, including arrhythmia (73). Therefore, additional research of dose-response and dose-toxicity relationships and further evaluation of the effects of neuronal TFEB activation, which reduces hyperphosphorylated tau accumulation and tauopathy, are needed before initiating clinical trials.

Our study highlights the therapeutic potential of ouabain for AD treatment by reduced hyper-phosphorylated tau accumulation and tauopathy through neuronal TFEB activation.

Activation of cell clearance due to TFEB activators further clarifies the roles of TFEB activation and the autophagy-lysosome system in the accumulation of abnormal protein, such as tau aggregates, and it indicates a new therapeutic strategy for AD (26). The results of this study advance the development of a viable pharmacological strategy to treat AD and neurodegenerative diseases by reducing tau via TFEB-induced autophagy.

References

1. Grundke-Iqbal, I., Iqbal, K., Tung, Y. C., Quinlan, M., Wisniewski, H. M., and Binder, L. I. (1986) Abnormal phosphorylation of the microtubule-associated protein tau (tau) in Alzheimer cytoskeletal pathology. *Proceedings of the National Academy of Sciences of the United States of America* **83**, 4913-4917

2. Gerson, J. E., and Kayed, R. (2013) Formation and propagation of tau oligomeric seeds. *Frontiers in neurology* **4**, 93

3. Boutajangout, A., Sigurdsson, E. M., and Krishnamurthy, P. K. (2011) Tau as a therapeutic target for Alzheimer's disease. *Current Alzheimer research* **8**, 666-677

4. Arriagada, P. V., Growdon, J. H., Hedley-Whyte, E. T., and Hyman, B. T. (1992) Neurofibrillary tangles but not senile plaques parallel duration and severity of Alzheimer's disease. *Neurology* **42**, 631-639

5. Gomez-Isla, T., Hollister, R., West, H., Mui, S., Growdon, J. H., Petersen, R. C., Parisi, J. E., and Hyman, B. T. (1997) Neuronal loss correlates with but exceeds neurofibrillary tangles in Alzheimer's disease. *Annals of neurology* **41**, 17-24

6. Weingarten, M. D., Lockwood, A. H., Hwo, S. Y., and Kirschner, M. W. (1975) A protein factor essential for microtubule assembly. *Proc Natl Acad Sci U S A* **72**, 1858-1862

7. Garg, S., Timm, T., Mandelkow, E. M., Mandelkow, E., and Wang, Y. (2011) Cleavage of Tau by calpain in Alzheimer's disease: the quest for the toxic 17 kD fragment. *Neurobiol Aging* **32**, 1-14

8. Derisbourg, M., Leghay, C., Chiappetta, G., Fernandez-Gomez, F. J., Laurent, C., Demeyer, D., Carrier, S., Buee-Scherrer, V., Blum, D., Vinh, J., Sergeant, N., Verdier,

Y., Buee, L., and Hamdane, M. (2015) Role of the Tau N-terminal region in microtubule stabilization revealed by new endogenous truncated forms. *Scientific reports* **5**, 9659

9. Wang, Y., and Mandelkow, E. (2015) Tau in physiology and pathology. *Nature Reviews Neuroscience* **17**, 22

10. Harada, A., Oguchi, K., Okabe, S., Kuno, J., Terada, S., Ohshima, T., Sato-Yoshitake, R., Takei, Y., Noda, T., and Hirokawa, N. (1994) Altered microtubule organization in small-calibre axons of mice lacking tau protein. *Nature* **369**, 488-491

11. DeVos, S. L., Goncharoff, D. K., Chen, G., Kebodeaux, C. S., Yamada, K., Stewart, F. R., Schuler, D. R., Maloney, S. E., Wozniak, D. F., Rigo, F., Bennett, C. F., Cirrito, J. R., Holtzman, D. M., and Miller, T. M. (2013) Antisense reduction of tau in adult mice protects against seizures. *The Journal of neuroscience : the official journal of the Society for Neuroscience* **33**, 12887-12897

12. Sievers, S. A., Karanicolas, J., Chang, H. W., Zhao, A., Jiang, L., Zirafi, O., Stevens, J. T., Münch, J., Baker, D., and Eisenberg, D. (2011) Structure-based design of non-natural amino-acid inhibitors of amyloid fibril formation. *Nature* **475**, 96-100

13. Lovestone, S., Boada, M., Dubois, B., Hull, M., Rinne, J. O., Huppertz, H. J., Calero, M., Andres, M. V., Gomez-Carrillo, B., Leon, T., and del Ser, T. (2015) A phase II trial of tideglusib in Alzheimer's disease. *Journal of Alzheimer's disease : JAD* **45**, 75-88

14. Boxer, A. L., Lang, A. E., Grossman, M., Knopman, D. S., Miller, B. L., Schneider, L. S., Doody, R. S., Lees, A., Golbe, L. I., Williams, D. R., Corvol, J. C., Ludolph, A., Burn, D., Lorenzl, S., Litvan, I., Roberson, E. D., Hoglinger, G. U., Koestler, M., Jack, C. R., Jr., Van Deerlin, V., Randolph, C., Lobach, I. V., Heuer, H. W., Gozes, I., Parker, L., Whitaker, S., Hirman, J., Stewart, A. J., Gold, M., and Morimoto, B. H. (2014)

Davunetide in patients with progressive supranuclear palsy: a randomised, double-blind, placebo-controlled phase 2/3 trial. *The Lancet. Neurology* **13**, 676-685

15. Brunden, K. R., Zhang, B., Carroll, J., Yao, Y., Potuzak, J. S., Hogan, A. M., Iba, M., James, M. J., Xie, S. X., Ballatore, C., Smith, A. B., 3rd, Lee, V. M., and Trojanowski, J. Q. (2010) Epothilone D improves microtubule density, axonal integrity, and cognition in a transgenic mouse model of tauopathy. *The Journal of neuroscience : the official journal of the Society for Neuroscience* **30**, 13861-13866

16. Asuni, A. A., Boutajangout, A., Quartermain, D., and Sigurdsson, E. M. (2007) Immunotherapy targeting pathological tau conformers in a tangle mouse model reduces brain pathology with associated functional improvements. *The Journal of neuroscience : the official journal of the Society for Neuroscience* **27**, 9115-9129

17. Sigurdsson, E. M. (2014) Tau immunotherapy and imaging. *Neuro-degenerative diseases* **13**, 103-106

18. Karagoz, G. E., Duarte, A. M., Akoury, E., Ippel, H., Biernat, J., Moran Luengo, T., Radli, M., Didenko, T., Nordhues, B. A., Veprintsev, D. B., Dickey, C. A., Mandelkow, E., Zweckstetter, M., Boelens, R., Madl, T., and Rudiger, S. G. (2014) Hsp90-Tau complex reveals molecular basis for specificity in chaperone action. *Cell* **156**, 963-974

19. Kruger, U., Wang, Y., Kumar, S., and Mandelkow, E. M. (2012) Autophagic degradation of tau in primary neurons and its enhancement by trehalose. *Neurobiol Aging* **33**, 2291-2305

20. Blair, L. J., Sabbagh, J. J., and Dickey, C. A. (2014) Targeting Hsp90 and its co-chaperones to treat Alzheimer's disease. *Expert opinion on therapeutic targets* **18**, 1219-1232

21. Harris, H., and Rubinsztein, D. C. (2011) Control of autophagy as a therapy for

neurodegenerative disease. *Nature reviews. Neurology* **8**, 108-117

22. Das, G., Shravage, B. V., and Baehrecke, E. H. (2012) Regulation and Function of Autophagy during Cell Survival and Cell Death. *Cold Spring Harbor perspectives in biology* **4**, 10.1101/cshperspect.a008813 a008813

23. Yoon, S. Y., and Kim, D. H. (2016) Alzheimer's disease genes and autophagy. *Brain research* **1649**, 201-209

24. Orr, M. E., and Oddo, S. (2013) Autophagic/lysosomal dysfunction in Alzheimer's disease. *Alzheimer's Research & Therapy* **5**, 53-53

25. Nixon, R. A. (2013) The role of autophagy in neurodegenerative disease. *Nature Medicine* **19**, 983

26. Polito, V. A., Li, H., Martini-Stoica, H., Wang, B., Yang, L., Xu, Y., Swartzlander, D. B., Palmieri, M., di Ronza, A., Lee, V. M. Y., Sardiello, M., Ballabio, A., and Zheng, H. (2014) Selective clearance of aberrant tau proteins and rescue of neurotoxicity by transcription factor EB. *EMBO Molecular Medicine* **6**, 1142-1160

27. Decressac, M., Mattsson, B., Weikop, P., Lundblad, M., Jakobsson, J., and Björklund, A. (2013) TFEB-mediated autophagy rescues midbrain dopamine neurons from α-synuclein toxicity. *Proceedings of the National Academy of Sciences of the United States of America* **110**, E1817-E1826

28. Sardiello, M., Palmieri, M., di Ronza, A., Medina, D. L., Valenza, M., Gennarino, V. A., Di Malta, C., Donaudy, F., Embrione, V., Polishchuk, R. S., Banfi, S., Parenti, G., Cattaneo, E., and Ballabio, A. (2009) A gene network regulating lysosomal biogenesis and function. *Science (New York, N.Y.)* **325**, 473-477

29. Settembre, C., Di Malta, C., Polito, V. A., Garcia Arencibia, M., Vetrini, F., Erdin, S.,

Erdin, S. U., Huynh, T., Medina, D., Colella, P., Sardiello, M., Rubinsztein, D. C., and Ballabio, A. (2011) TFEB links autophagy to lysosomal biogenesis. *Science (New York, N.Y.)* **332**, 1429-1433

30. Medina, D. L., Di Paola, S., Peluso, I., Armani, A., De Stefani, D., Venditti, R., Montefusco, S., Scotto-Rosato, A., Prezioso, C., Forrester, A., Settembre, C., Wang, W., Gao, Q., Xu, H., Sandri, M., Rizzuto, R., De Matteis, M. A., and Ballabio, A. (2015) Lysosomal calcium signalling regulates autophagy through calcineurin and TFEB. *Nature cell biology* **17**, 288-299

31. Xiao, Q., Yan, P., Ma, X., Liu, H., Perez, R., Zhu, A., Gonzales, E., Tripoli, D. L., Czerniewski, L., Ballabio, A., Cirrito, J. R., Diwan, A., and Lee, J. M. (2015) Neuronal-Targeted TFEB Accelerates Lysosomal Degradation of APP, Reducing Abeta Generation and Amyloid Plaque Pathogenesis. *The Journal of neuroscience : the official journal of the Society for Neuroscience* **35**, 12137-12151

32. Gong, C. X., Lidsky, T., Wegiel, J., Zuck, L., Grundke-Iqbal, I., and Iqbal, K. (2000) Phosphorylation of microtubule-associated protein tau is regulated by protein phosphatase 2A in mammalian brain. Implications for neurofibrillary degeneration in Alzheimer's disease. *The Journal of biological chemistry* **275**, 5535-5544

33. Gong, C. X., Wang, J. Z., Iqbal, K., and Grundke-Iqbal, I. (2003) Inhibition of protein phosphatase 2A induces phosphorylation and accumulation of neurofilaments in metabolically active rat brain slices. *Neuroscience letters* **340**, 107-110

34. Mucke, L., and Selkoe, D. J. (2012) Neurotoxicity of amyloid beta-protein: synaptic and network dysfunction. *Cold Spring Harbor perspectives in medicine* **2**, a006338

35. Kamat, P. K., and Nath, C. (2015) Okadaic acid: a tool to study regulatory mechanisms for neurodegeneration and regeneration in Alzheimer's disease. *Neural*

regeneration research **10**, 365-367

36. Osseo-Asare, A. D. (2008) Bioprospecting and Resistance: Transforming Poisoned Arrows into Strophantin Pills in Colonial Gold Coast, 1885–1922. *Social History of Medicine* **21**, 269-290

37. Song, H.-L., Shim, S., Kim, D.-H., Won, S.-H., Joo, S., Kim, S., Jeon, N. L., and Yoon, S.-Y. (2014) β-Amyloid is transmitted via neuronal connections along axonal membranes. *Annals of neurology* **75**, 88-97

38. Wang, C., Niederstrasser, H., Douglas, P. M., Lin, R., Jaramillo, J., Li, Y., Olswald, N. W., Zhou, A., McMillan, E. A., Mendiratta, S., Wang, Z., Zhao, T., Lin, Z., Luo, M., Huang, G., Brekken, R. A., Posner, B. A., MacMillan, J. B., Gao, J., and White, M. A. (2017) Small-molecule TFEB pathway agonists that ameliorate metabolic syndrome in mice and extend C. elegans lifespan. *Nature communications* **8**, 2270

39. Spires, T. L., Orne, J. D., SantaCruz, K., Pitstick, R., Carlson, G. A., Ashe, K. H., and Hyman, B. T. (2006) Region-specific dissociation of neuronal loss and neurofibrillary pathology in a mouse model of tauopathy. *The American journal of pathology* **168**, 1598-1607

40. de Calignon, A., Fox, L. M., Pitstick, R., Carlson, G. A., Bacskai, B. J., Spires-Jones, T. L., and Hyman, B. T. (2010) Caspase activation precedes and leads to tangles. *Nature* **464**, 1201-1204

41. Kopeikina, K. J., Carlson, G. A., Pitstick, R., Ludvigson, A. E., Peters, A., Luebke, J. I., Koffie, R. M., Frosch, M. P., Hyman, B. T., and Spires-Jones, T. L. (2011) Tau accumulation causes mitochondrial distribution deficits in neurons in a mouse model of tauopathy and in human Alzheimer's disease brain. *The American journal of pathology* **179**, 2071-2082

42. Yamada, M., Hayashida, M., Zhao, Q., Shibahara, N., Tanaka, K., Miyata, T., and Matsumoto, K. (2011) Ameliorative effects of yokukansan on learning and memory deficits in olfactory bulbectomized mice. *Journal of ethnopharmacology* **135**, 737-746

43. Pena-Llopis, S., Vega-Rubin-de-Celis, S., Schwartz, J. C., Wolff, N. C., Tran, T. A., Zou, L., Xie, X. J., Corey, D. R., and Brugarolas, J. (2011) Regulation of TFEB and V-ATPases by mTORC1. *The EMBO journal* **30**, 3242-3258

44. Kim, S., Choi, K. J., Cho, S. J., Yun, S. M., Jeon, J. P., Koh, Y. H., Song, J., Johnson, G. V., and Jo, C. (2016) Fisetin stimulates autophagic degradation of phosphorylated tau via the activation of TFEB and Nrf2 transcription factors. *Scientific reports* **6**, 24933

45. Yoon, S. Y., Choi, J. E., Kweon, H. S., Choe, H., Kim, S. W., Hwang, O., Lee, H., Lee, J. Y., and Kim, D. H. (2008) Okadaic acid increases autophagosomes in rat neurons: implications for Alzheimer's disease. *Journal of neuroscience research* **86**, 3230-3239

46. Korolchuk, V. I., Menzies, F. M., and Rubinsztein, D. C. (2009) A novel link between autophagy and the ubiquitin-proteasome system. *Autophagy* **5**, 862-863

47. Vabulas, R. M., and Hartl, F. U. (2005) Protein synthesis upon acute nutrient restriction relies on proteasome function. *Science (New York, N.Y.)* **310**, 1960-1963

48. Ciechanover, A., Orian, A., and Schwartz, A. L. (2000) Ubiquitin-mediated proteolysis: biological regulation via destruction. *BioEssays : news and reviews in molecular, cellular and developmental biology* **22**, 442-451

49. Corradetti, M. N., and Guan, K. L. (2006) Upstream of the mammalian target of rapamycin: do all roads pass through mTOR? *Oncogene* **25**, 6347-6360

50. Settembre, C., Zoncu, R., Medina, D. L., Vetrini, F., Erdin, S., Erdin, S., Huynh, T.,

Ferron, M., Karsenty, G., Vellard, M. C., Facchinetti, V., Sabatini, D. M., and Ballabio, A. (2012) A lysosome-to-nucleus signalling mechanism senses and regulates the lysosome via mTOR and TFEB. *The EMBO journal* **31**, 1095-1108

51. Magnaudeix, A., Wilson, C. M., Page, G., Bauvy, C., Codogno, P., Lévêque, P., Labrousse, F., Corre-Delage, M., Yardin, C., and Terro, F. (2013) PP2A blockade inhibits autophagy and causes intraneuronal accumulation of ubiquitinated proteins. *Neurobiology of Aging* **34**, 770-790

52. Shulman, J. M., and Feany, M. B. (2003) Genetic modifiers of tauopathy in Drosophila. *Genetics* **165**, 1233-1242

53. Tognon, E., Kobia, F., Busi, I., Fumagalli, A., De Masi, F., and Vaccari, T. (2016) Control of lysosomal biogenesis and Notch-dependent tissue patterning by components of the TFEB-V-ATPase axis in Drosophila melanogaster. *Autophagy* **12**, 499-514

54. Lewis, J., McGowan, E., Rockwood, J., Melrose, H., Nacharaju, P., Van Slegtenhorst, M., Gwinn-Hardy, K., Paul Murphy, M., Baker, M., Yu, X., Duff, K., Hardy, J., Corral, A., Lin, W. L., Yen, S. H., Dickson, D. W., Davies, P., and Hutton, M. (2000) Neurofibrillary tangles, amyotrophy and progressive motor disturbance in mice expressing mutant (P301L) tau protein. *Nature genetics* **25**, 402-405

55. Le Corre, S., Klafki, H. W., Plesnila, N., Hubinger, G., Obermeier, A., Sahagun, H., Monse, B., Seneci, P., Lewis, J., Eriksen, J., Zehr, C., Yue, M., McGowan, E., Dickson, D. W., Hutton, M., and Roder, H. M. (2006) An inhibitor of tau hyperphosphorylation prevents severe motor impairments in tau transgenic mice. *Proceedings of the National Academy of Sciences of the United States of America* **103**, 9673-9678

56. Hamlyn, J. M., and Blaustein, M. P. (2016) Endogenous Ouabain: Recent Advances

and Controversies. *Hypertension (Dallas, Tex. : 1979)* **68**, 526-532

57. Furstenwerth, H. (2010) Ouabain - the insulin of the heart. *International journal of clinical practice* **64**, 1591-1594

58. Manunta, P., Ferrandi, M., Bianchi, G., and Hamlyn, J. M. (2009) Endogenous ouabain in cardiovascular function and disease. *Journal of hypertension* **27**, 9-18

59. Hamlyn, J. M., Blaustein, M. P., Bova, S., DuCharme, D. W., Harris, D. W., Mandel, F., Mathews, W. R., and Ludens, J. H. (1991) Identification and characterization of a ouabain-like compound from human plasma. *Proceedings of the National Academy of Sciences of the United States of America* **88**, 6259-6263

60. Rana, S., Rajakumar, A., Geahchan, C., Salahuddin, S., Cerdeira, A. S., Burke, S. D., George, E. M., Granger, J. P., and Karumanchi, S. A. (2014) Ouabain inhibits placental sFlt1 production by repressing HSP27-dependent HIF-1alpha pathway. *FASEB journal : official publication of the Federation of American Societies for Experimental Biology* **28**, 4324-4334

61. Ninsontia, C., and Chanvorachote, P. (2014) Ouabain mediates integrin switch in human lung cancer cells. *Anticancer research* **34**, 5495-5502

62. Dvela-Levitt, M., Ami, H. C., Rosen, H., Shohami, E., and Lichtstein, D. (2014) Ouabain improves functional recovery following traumatic brain injury. *Journal of neurotrauma* **31**, 1942-1947

63. Felippe Goncalves-de-Albuquerque, C., Ribeiro Silva, A., Ignacio da Silva, C., Caire Castro-Faria-Neto, H., and Burth, P. (2017) Na/K Pump and Beyond: Na/K-ATPase as a Modulator of Apoptosis and Autophagy. *Molecules (Basel, Switzerland)* **22**

64. Liu, Y., and Levine, B. (2015) Autosis and autophagic cell death: the dark side of

autophagy. *Cell death and differentiation* **22**, 367-376

65. Garcia, D. G., de Castro-Faria-Neto, H. C., da Silva, C. I., de Souza e Souza, K. F., Goncalves-de-Albuquerque, C. F., Silva, A. R., de Amorim, L. M., Freire, A. S., Santelli, R. E., Diniz, L. P., Gomes, F. C., Faria, M. V., and Burth, P. (2015) Na/K-ATPase as a target for anticancer drugs: studies with perillyl alcohol. *Molecular cancer* **14**, 105

66. Trenti, A., Grumati, P., Cusinato, F., Orso, G., Bonaldo, P., and Trevisi, L. (2014) Cardiac glycoside ouabain induces autophagic cell death in non-small cell lung cancer cells via a JNK-dependent decrease of Bcl-2. *Biochemical pharmacology* **89**, 197-209

67. Roczniak-Ferguson, A., Petit, C. S., Froehlich, F., Qian, S., Ky, J., Angarola, B., Walther, T. C., and Ferguson, S. M. (2012) The Transcription Factor TFEB Links mTORC1 Signaling to Transcriptional Control of Lysosome Homeostasis. *Science signaling* **5**, ra42-ra42

68. Martina, J. A., Chen, Y., Gucek, M., and Puertollano, R. (2012) MTORC1 functions as a transcriptional regulator of autophagy by preventing nuclear transport of TFEB. *Autophagy* **8**, 903-914

69. Selvakumar, P., Owens, T. A., David, J. M., Petrelli, N. J., Christensen, B. C., Lakshmikuttyamma, A., and Rajasekaran, A. K. (2014) Epigenetic silencing of Na,K-ATPase beta 1 subunit gene ATP1B1 by methylation in clear cell renal cell carcinoma. *Epigenetics* **9**, 579-586

70. Durlacher, C. T., Chow, K., Chen, X. W., He, Z. X., Zhang, X., Yang, T., and Zhou, S. F. (2015) Targeting Na(+)/K(+) -translocating adenosine triphosphatase in cancer treatment. *Clinical and experimental pharmacology & physiology* **42**, 427-443

71. Liu, L., Wu, J., and Kennedy, D. J. (2016) Regulation of Cardiac Remodeling by

Cardiac Na(+)/K(+)-ATPase Isoforms. *Frontiers in physiology* **7**, 382

72. Simpson, C. D., Mawji, I. A., Anyiwe, K., Williams, M. A., Wang, X., Venugopal, A. L., Gronda, M., Hurren, R., Cheng, S., Serra, S., Beheshti Zavareh, R., Datti, A., Wrana, J. L., Ezzat, S., and Schimmer, A. D. (2009) Inhibition of the sodium potassium adenosine triphosphatase pump sensitizes cancer cells to anoikis and prevents distant tumor formation. *Cancer research* **69**, 2739-2747

73. Melero, P. C., Medarde, M., and San Feliciano, A. (2000) A Short Review on Cardiotonic Steroids and Their Aminoguanidine Analogues. *Molecules (Basel, Switzerland)* **5**

국문 초록

서론: 알츠하이머 병 (Alzheimer's disease; AD)의 주요 병원성 분자 중 하나인 신경원섬유얽힘 (Neurofibrillary tangles; NFTs)는 비정상적으로 과인산화 된 독성 타우 (Tau) 단백질의 축적에 의해 형성한다. 또 다른 주요 병원성 분자인 아밀로이드 베타 (Amyloid beta; Aβ)를 표적으로 하는 치료제의 거의 모든 시도가 실패하고, 실제 환자에서 신경원섬유얽힘 진행 과정이 알츠하이머 병의 병리 증상 기준이 되는 Braak stage와 일치를 보임에 따라 타우 단백질이 치료 표적으로 떠오르고 있다. 타우 단백질의 직접적 치료 방법 중 하나로 세포 내 프로테아좀 (Proteasome; 단백질분해효소복합체)이나 자가포식 (Autophagy) 자극을 통한 독성 타우 단백질의 제거가 있는데, 실제 알츠하이머 환자 뇌에서 자가포식소체 (Autophagosome)의 축적과 라이소솜의 기능장애 (Lysosomal dysfunction)가 확인되고 있어 치료 전략으로 기대가 높다. 전사조절인자EB (Transcription factor EB; TFEB)의 활성화는 자가포식과 라이소솜 과정을 자극시키므로 이를 통한 독성 타우 단백질의 제거를 기대한다. 오카다익산 (Okadaic acid; OA) 는 신경세포에서 타우를 과인산화시키고 신경세포의 퇴행과 시냅스 손실 등과 같이 알츠하이머 병과 유사한 생체 내 병리학 적 진행을 유도하기에 독성 타우 단백질에 대한 신경퇴행 질병 연구 모델로 유용하다.

목적: 본 연구는 타우에 의해 유도되는 세포손상에 대한 신경보호와 전사인자 EB를 활성화 시키는 물질을 발굴하고 이 물질의 신경보호 효과와 타우의 효과적인 억제를 확인하여 그 메커니즘을 규명하고자 한다.

결론: 본 연구는, 1) 오카다익산에 의한 과인산 타우 관련 신경 퇴행 모델에서 신경세포 보호 효과와 2) 세포질에서 핵으로 위치 이동되는 TFEB의 활성화를 타겟으로 스크리닝을 진행 하여 공통으로 활성을 보인 화합물, 와베인(ouabain)을 확인하였다. 신경세포 독성 및 생존력에 대한 실험에서 와베인은 오카다익산 유발 신경퇴행 모델에서 유의하게 신경 세포 보호 효과를 보였다. 와베인은 TFEB을 세포질에서 핵으로 전위시키고 LAMP1과 LC3B 같은 자가포식-라이소솜 관련 단백질을 활성화 하였다. 타우

과발현 된 SH-SY5Y와 신경세포에서 와베인 처리는 인산화된 타우 (Ser199 / 202 및 Ser396 영역)의 감소를 야기했는데, 라이소솜 억제제인 bafilomycin A1 (10 nM, 4 h)과 와베인 처리 하에서 인산화 타우 감소가 차단되는 결과들은 와베인의 독성 타우 인산화의 분해 과정이 자가포식 경로를 통한다는 것을 의미한다. 또한, 인산화 된 4EBP1과 p70S6-kinase는 와베인 처리 시간과 용량 의존적으로 유의하게 감소를 보였는데 이러한 결과는 와베인이 mTORC1 억제를 통해 TFEB의 탈인산화 및 자가포식 과정의 활성화에 관여한다는 것을 의미한다. human-타우가 발현할 경우 무질서하고 융합된 거친 눈 표현형을 나타내는 초파리 모델 실험에서, 와베인 섭취 그룹의 명확하게 잘 조직 된 눈 표현형과 타우 인산화 단백질 양의 감소가 보였다. 또, P301L 돌연변이가 있는 human-타우를 발현하며 연령에 따른 타우 병리학, 신경세포 변성 및 점진적 기억력 결핍을 나타내는 TauP301L생쥐 실험은 6 주간 와베인이 투여된 그룹에서 인지 및 기억의 향상과 인산화된 타우의 감소를 검증했다.

토의: 본 연구에서는 심장 배당체로 알려진 와베인을 이용하여 오카다익산 유발 신경퇴행모델에서 세포 보호 효과 및 TFEB의 활성화를 통한 자가포식-라이소솜 관련 단백질의 증가와 이에 따른 인산화된 타우 단백질의 감소를 확인하였다. 이러한 결과들은 세포 실험과 동물 실험에서 직접적으로 확인되었으며, 이는 TFEB의 활성화가 자가포식을 통해 세포독성 타우를 감소시켜 알츠하이머 병 및 신경 퇴행성 질환을 치료할 수 있는 약리학적 전략 발전에 의의가 있다.